6-2013

Electrospun Plant Protein Scaffolds with Fibers Oriented Randomly and Evenly in Three-Dimensions for Soft Tissue Engineering Applications

Shaobo Cai
University of Nebraska-Lincoln, caishaobo2005@gmail.com

Electrospun Plant Protein Scaffolds with Fibers Oriented Randomly and Evenly in Three-Dimensions for Soft Tissue Engineering Applications

by

Shaobo Cai

A THESIS

Presented to the Faculty of

The Graduate College at the University of Nebraska

In Partial Fulfillment of Requirements

For the Degree of Master of Science

Major: Textiles, Merchandising and Fashion Design

Under the Supervision of Professor Yiqi Yang

Lincoln, NE

July, 2013

Electrospun Plant Protein Scaffolds with Fibers Oriented Randomly and Evenly in Three-Dimensions for Soft Tissue Engineering Applications

Shaobo Cai, M.S.

University of Nebraska, 2013

Advisor: Yiqi Yang

In this work, electrospinnable and water stable soyprotein was extracted by using a reducing agent in mild alkaline condition, and novel 3D zein and 3D pure soyprotein electrospun scaffolds with three-dimensionally and randomly oriented fibers and large interconnected pores were successfully fabricated by reducing surface resistivity of materials. This unique structure is different from most electrospun scaffolds with fibers oriented mainly in one direction. The structure of novel 3D scaffolds could more closely mimic the 3D randomly oriented fibrous architectures in many native extracellular matrixes (ECM). Confocal laser scanning microscope shows that instead of becoming flattened cells when cultured in conventional electrospun scaffolds, the cells cultured on novel 3D scaffolds could develop into stereoscopic topographies, which highly simulated in vivo 3D cellular morphologies and are believed to be of vital importance for cells to function and differentiate appropriately. *In vitro* cell attachment, proliferation and differentiation study indicated that the 3D fibrous scaffold could better support the attachment and proliferation of NIH 3T3 mouse fibroblast cells, and could better support ADMSC for proliferation and adipogenic differentiation. One mechanism of this fabrication

process has also been proposed and shown that the rapid delivery of electrons on the fibers was the crucial factor for formation of 3D architectures. The novel dissolution method could be applied to a number of water stable proteins that contains large amount of intermolecular and intramolecular disulfide bond crosslinkages, and 3D electrospinning method could be applied to many other proteins and materials.

Acknowledgements

First, I am sincerely grateful to my advisor Dr. Yiqi Yang for his encouragement, thoughtful insight and precious guidance during my research. I benefited from his advices throughout my study in UNL.

I would like to express my sincere gratitude to Dr. Narendra Reddy for his valuable guidance and great help. I am deeply thankful to my committee member Dr. Shubha Bennur for dedicating her time to evaluate my work.

I am also grateful for Helan Xu, who has been an invaluable member of my research. I am deeply appreciative of her efforts and great help for my research. I'd also like to thank Qiuran Jiang; I learned a lot of experimental methods from her, especially in cell culture area.

I would like also to deeply thank all of my other fellow lab mates and friends with whom I have shared many wonderful experiences with. Besides being great to work with, my lab mates have always been a lot of fun to be around and I have a lot of happy memories with them.

Finally I would like to give my special thanks to my parents who have always supported me in everything. Thank you for your love and support.

Table of Contents

CHAPTER 1: INTRODUCTION

Soft Tissue Engineering

1.1. Soft Tissue Engineering

Tissue engineering is the use of a combination of cells, engineering and materials methods, and suitable biochemical factors to improve or replace biological functions. [1] In this technology, tissue engineering scaffolds serve as a temporary artificial extracellular matrix (ECM) to support the growth of cells during the formation of neo-tissues/organs *in vitro* or *in vivo*, and determine the success of regenerating neo-tissues/organs by their properties. [2-4]

In practice, the term is closely associated with applications that repair or replace portions of or whole tissues, such as bone, cartilage or soft tissues. [5] The term soft tissue refers to tissues that connect, support, or surround other structures and organs of the body. [6] Soft tissue includes tendons, ligaments, fibrous tissues, fat, and muscles, nerves and blood vessels. [7] In this work, fat tissue was closed as an example of soft tissues for regeneration study.

Conventional soft tissue-grafting procedures have had some clinical success for soft tissue augmentation and reconstruction. [8-10] However, the need for secondary surgical procedures to harvest autologous tissues and an average of 40–60% reduction in graft volume over time are considered drawbacks of current autologous fat transplantation procedures. [11] It should be possible to overcome these problems with tissue-engineered soft tissue grafts generated from the patient's own adult stem cells. [12-14] The use of human adipose tissue-derived adult stem cells

(ADSCs) as a source of cells for therapeutic applications has many potential advantages. [15] For adipose tissue engineering, the use of ADSCs may be more useful than differentiated adipocytes because mature adipocytes have low expandability and poor ability for volume retention following in vivo soft tissue reconstruction. [16] ADSCs are highly expandable in culture and can be readily induced to differentiate into adipose tissue-forming cells by exposure to a well-established adipogenic medium. [17, 18]

Biomedical Scaffolds

1.2. Biomedical Scaffolds

Scaffolds, in biomedical area, are artificial substance with cells implanted or 'seeded' onto them to support tissue formation. [19] Scaffolds usually serve at least one of the following purposes: improve cell's attachment and migration, deliver and retain biochemical factors, enable diffusion of vital cell nutrients and expressed products, or exert certain mechanical and biological influences to modify the behavior of the cell phase. [20] The material and structure of scaffolds are crucial for cell-scaffold and cell-cell interactions.

Based on whether development of cells in the vertical or thickness directions could be supported, scaffolds could be categorized into two dimensional and three dimensional architectures. 2D scaffolds, such as film, are not applicable for soft tissue engineering. Differentiated adipocyte cells will lose their round adipogenic phenotypes and turn into spindle fibroblast shapes. [21] Three dimensional scaffolds could be categorized into non-fibrous and fibrous structures. Non-fibrous scaffolds are mainly composed of solid walled structures in three dimensions. They can be fabricated via porogens leaching method, freeze drying method and polymerization method.

Fibrous scaffolds are mainly composed of nano or submicron fibers in three dimensionally random orientations. Self assembly, phase separation and electrospinning are three major methods to produce 3D fibrous structures. Self assembly is a bottom-up method to build polymers from monomers and therefore is not applicable for macromolecules. Phase separation is only applicable to certain types of polymers that can be dissolved or exchanged in easily freezable solvents, and shows little control on the morphologies of the fibers. [22]

Ideal tissue engineering scaffolds should be capable of closely mimicking the topographies and spatial structures of native ECMs to facilitate cells to grow and differentiate following the patterns similar to that found in native tissues and organs. [23-25] Morphologies of ECMs vary according to functions of target tissues and cell types in the tissues. For example, in skin tissue, the top layer is formed by compact packing of epithelial cells on a two dimensional (2D) fibrous ECM basement membrane. [26, 27] Three-dimensional spatial spreading of fibroblasts and immune cells occurs in the interior region of the skin tissue, and correspondingly the ECMs are constructed by stereoscopically and randomly oriented ultrafine protein fibers. [28, 29] Fibrous structures with 3D orientation and random distribution can also be found in native ECMs in breast, liver, bladder, lung and many other organs and tissues. [30, 31] It has been reported that cells cultured on flat 2D substrates may differ considerably in morphology and differentiation pattern from those cultured in more physiological 3D environments. [32-34] Therefore, it is reasonable to fabricate scaffolds with particular morphology and structure according to categories and functions of original native tissues.

Thus, among the different shapes, fibrous scaffolds are preferred for tissue engineering. So far, electrospinning, self-assembly and phase separation have been the most common approaches to produce fibrous 3D scaffolds. Electrospinning is a common method to process various types of natural and synthetic polymers.

Electrospun Scaffolds

1.3. Electrospun Scaffolds

The electrospining method could produce fibrous scaffolds with diameters ranging from nanometer to micron. [35] However, for conventional electrospining, the fibers only randomly orient in 2D but not in the thickness direction. [36-37] The limitation of the 2D fibrous scaffolds is similar to that of a film, in a 2D electrospining scaffolds, vertical penetration and development of cells is restricted due to the tight packing of fiber mats. [38, 39]

To overcome these shortcomings, efforts have been made to develop 3D fibrous structures via electrospinning. Most of the modification involved physical blocking of fiber packing during the collection process. Coagulation bath, porogens spraying and coarse fiber incorporation are employed to increase the thickness and porosity of electrospun fibrous mats. [40-44] However, since the fabrication mechanism of electrospun fibers with 2D orientation has not been changed, 3D fibrous scaffolds made from modified electrospinning methods did not show the architecture of spatial and three dimensional orientations of fibers.

Materials for Fabricating Biomedical Scaffolds

1.4. Materials for Fabricating Biomedical Scaffolds

Natural materials include collagen, fibrin, hyaluronic acid and chitosan have been made into many kinds of scaffolds including sponges, hydrogel and fibrous scaffolds. The advantages of natural materials are their preferable biocompatibility and biodegradability. [45] They are either components of native ECMs or have high similarity to the native ECM components. For example, collagen, fibrin and HA are found in the native ECM, while chitosan shows high molecular and structural similarity to the HA. [46]

However, many currently commonly used nature materials, such as collagen, silk fibroin and gelatin, have several limitations that limit their use in medical applications. Firstly, the scaffolds from natural materials demonstrate poor mechanical properties, poor dimensional stability and fast degradation due to the existence of the relevant enzymes in body. [47] Second, collagen and many other animal source proteins, such as keratin and bull serum, have the risk of transmit zoonotic viruses. [48] Silk fibroin has long degradation rates that make it unsuitable for short term applications, and it has been recently discovered that silk fibroin may cause amyloidosis, a chronic inflammatory reaction. [49] Hydrolyzed animal sources proteins, such as gelatin, and or some other proteins, like zein, do not transmit viruses or cause inflammatory reactions. However, both gelatin and zein has poor water stability and unsatisfied mechanical properties, and cannot be used in aqueous environment without further crosslinking or blending with other polymers. [50] The cross-linking or blending process may alter the biocompatibility and biodegradability of nature proteins. For example, blending polymers with high hydrophobicity or poor degradability may cause undesirable changes to the surface properties and the biodegradability of the natural protein materials. [51] Cross-linking has been used as alternatives to polymer blending. However,

most cross-linking agents are toxic and expensive, and therefore cross-linking may decrease the biocompatibility and increase cytotoxicity of natural protein materials. [52]

Synthetic polymers have also been made into tissue engineering scaffolds for soft tissue repairing. Polycaprolactone, polyethylene glycol diacrylate and poly-lactic-co-glycolic acid are typical examples. These scaffolds are usually featured for their good mechanical properties. However, due to the lack of bio-signaling moieties, cells do not tend to adhere and proliferate in the synthetic polymer based scaffolds. [53] Furthermore, the degradation products from the synthetic polymers are highly acidic and can cause death of cells and inflammatory and immune response in body. [54]

As plant proteins, zein, soyprotein does not transmit zoonotic diseases and has been proved possess good biocompatibility. For soyprotein, it also has controllable degradability, satisfying water stability and mechanical properties. So far, zein has been electrospun into 2D ultra-fine fibers for biomedical applications, pure soyprotein electrospun ultra-fine fibers have not been reported yet. [55-57] The reason is that soyprotein does not dissolve in solvents commonly used for electrospinning and it has only been possible to develop soyprotein blended with PVA, zein or poly (ethylene oxide) into nanofiber by electrospinning. [56] Although it has been demonstrated that the soyprotein blended fibrous scaffolds have excellent potential for tissue engineering, blending soyprotein with other polymers reduces the biofunctionality of soyprotein. We believe that electrospun 3D scaffolds from zein and soyprotein would offer better alternatives for tissue engineering.

CHAPTER 2: OBJECTIVES

Overall Objective: Developing novel electrospun plant protein scaffolds with fibers oriented randomly and evenly in three-dimensions, and evaluating the ability of novel 3D scaffold for soft tissue engineering repairing. In detail, objectives include:

2.1. Extract soluble and electrospinnable soyprotein

2.2. Produce electrospun 100% soyprotein ultra-fine fibers

2.3. Investigate the water stability and cytocompatibility of soyprotein ultra-fine fibers.

2.4. Electrospinning zein and soyprotein scaffolds with fibers oriented randomly in 3D

2.5. Mechanism study of the formation process

2.6. Study the influence of scaffold topology on cell's proliferation and morphology

2.7. Study the ability of 3D soyprotein scaffold on supporting the adipogenic differentiation of ADMSCs

CHAPTER 3: LITERATURE REVIEW

Limitations of Current Three-dimensional Electrospun Scaffolds

3.1. Limitations of Current Three-dimensional Electrospun Scaffolds

To date, although numerous reports are available on developing 3D scaffolds by electrospinning, there has been limited success in obtaining scaffolds containing randomly oriented fibers that provide high porosity, pore size and allow cells to infiltrate into the scaffolds and have a true 3D architecture. Many 3D electrospinning techniques have been developed to fabricate electrospun scaffolds with larger pores and higher porosity to improve cell accessibility of the scaffolds, [41-44] however, to the best of our knowledge, no studies have reported the successful fabrication of scaffolds with three-dimensionally randomly oriented fibrous structures that could support cells to grow and spread in three-dimensions as seen in native ECMs. Cells cultured on current 3D scaffolds still tended to have flattened morphologies, and thus differed structurally from stereoscopically developed cells in many native tissues. [58]

In addition, the parallel fibrous layer-by-layer structures lead to difficulties in forming pores in thickness direction with sizes comparable to those in planar directions. Resultantly, the improvement of scaffold porosity is limited. [59, 60] The reason is that the basic principle of most current 3D electrospinning techniques, such as wet electrospinning, integration of coarse fibers electrospinning and electrospinning with porogens, is physical blocking. Coagulation bath, frameworks consisted of coarse fibers and porogenic agents, such as dry ice or sucrose, utilized in the above mentioned techniques could physically increase distance between the electrospun

fibers and have led to deeper penetration of cells into interior of scaffolds to some extent, but could not totally change the planar orientation of the electrospun fibers.

Limitations of Current Protein Based Scaffolds

3.2. Limitations of Current Protein Based Scaffolds

Protein-base materials have more similar molecule structure to the compositions of native extracellular matrix, and most of them have more favorable biocompatibility and biodegradability. However, many current-used proteins also have some disadvantages. Firstly, many animal source proteins, like keratin, collagen or bull serum albumin, have the potentials to provoke zoonotic diseases, such as bovine spongiform encephalopathy. Secondly, for hydrolyzed animal source proteins, gelatins, or some other proteins, like zein, their mechanical properties and water stability are unsatisfied, and need further cross-linking or blending with other polymers to be used for biomedical applications. The cross-linking or blending process may alter the biocapability and biodegradability of nature proteins.

Zein and soyprotein does not transmit zoonotic diseases and has been proved possess good biocompatibility. For soyprotein, it also has controllable degradability, satisfying water stability and mechanical properties. So far, zein has been electrospun into 2D ultra-fine fibers for biomedical applications, pure soyprotein electrospun ultra-fine fibers have not been reported yet, and only electrospun scaffolds from soyprotein blended with PVA, zein or poly (ethylene oxide) into nanofiber by electrospinning were reported. [45-47]

Limitations of Current Soyprotein Based Biomedical Scaffolds

3.3. Limitations of Current Soyprotein Based Biomedical Scaffolds

It is has also been reported that basal cell culture medium added soy peptides could significantly increase the proliferation of human adipose tissue-derived mesenchymal stem cells (ADSCs). [61] Therefore, in recent one or two years, there are more and more researches have been reported in utilizing soyprotein for tissue engineering applications. Till so far, pure soyprotein has been fabricated into films, sponges, normal fibers for bio-medical studies. Soyprotein ultrafine fibers have also only been fabricated by blending SPI with PEO or Zein.

Although several attempts had been made to produce pure soyprotein electrospun fibers, till now, no successful fabrication has been reported. This is because soyprotein is a globular protein, which contains many intermolecular and intramolecular disulfide bond crosslinkages which are stable in most common organic solvents, such as acetic acid, dimethylformamide (DMF), tetrahydrofuran (THF), that are suitable for electrospinning. [62-65] According to currently reported research, only HFIP and NaOH aqueous solution could dissolve soyprotein to form transparent solutions. [62] However, neither of these soyprotein solutions could be electrospun into ultra-fine fibers, without adding other polymers such as PEO and zein.

It is reported that by stirring the solution more than two weeks, soyprotein could be dissolved in HFIP. [63] However, this solution is still cannot be electrospun into ultrafine fibers, and only electrospraying occurred at lower concentrations and complete occlusion of the syringe needle occurred at higher concentrations. We believe in this solution, thought soyprotein seems has been dissolved, the molecule chains of soyprotein did not stretch into linear form, instead,

soyprotein molecule chains are still in the form of globular. The molecules cannot entangle with each other very well, therefore the spinning ability of the solution is quite low, and the solution cannot be spun into continues ultra-fine fibers. To improve the spinning ability of the solution, PEO and other polymers have to be added to increase the entanglement of molecules.

The other dissolution method for SPI is to use strong alkali condition to hydrolyze and break down SPI molecules chains into small fractions which are much easier to dissolve. However, this degradation process will also decrease the spinning ability of the solution, because the entanglement of the small fractions is also quite low. Similar with HFIP, SPI dissolved in alkaline solution could be used for electrospining only by blending SPI with other polymers, such as PEO or zein. [63] As mentioned above, the blending process may change the biocapability and biodegradability of SPI. Moreover, the water stability of the hydrolyzed soy proteins scaffold may also problematic, further crosslinking may be needed for many biomedical applications.

CHAPTER 4: MATERIALS, METHODS, AND PROCEDURES

General Research Design

4.1. General Research Design

The general research design shows in **Figure 1** and **Figure2**.

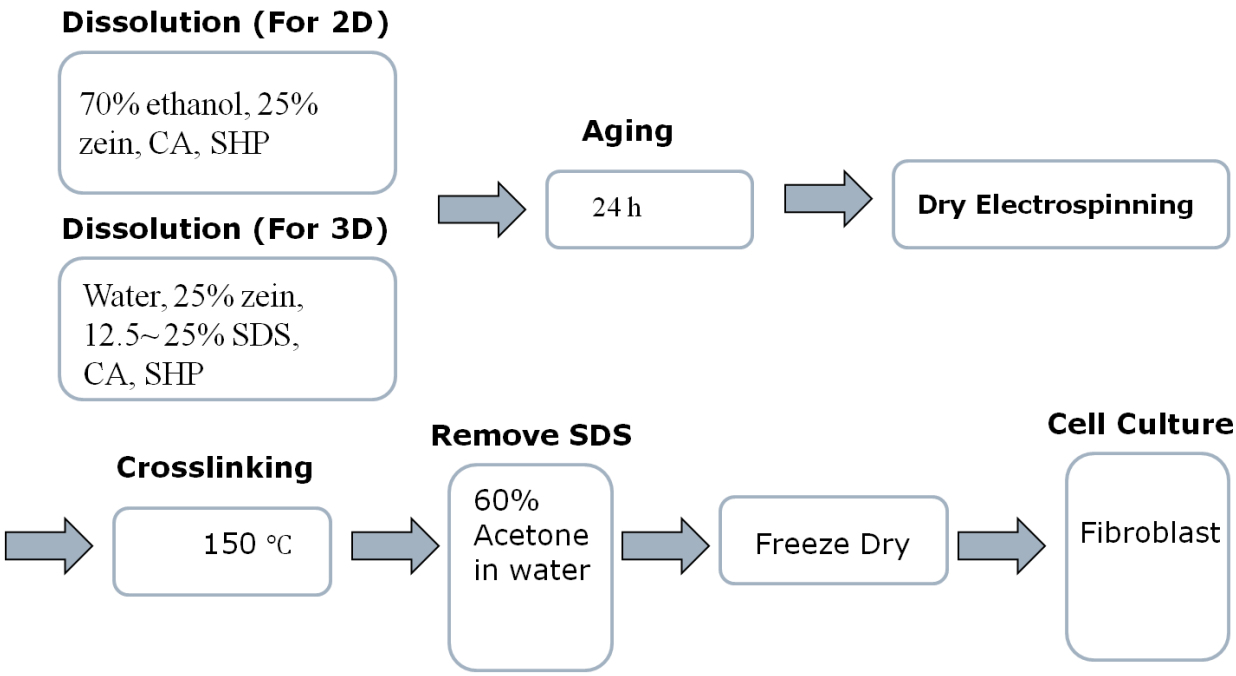

Figure 1 Fabrication process of zein 3D scaffold

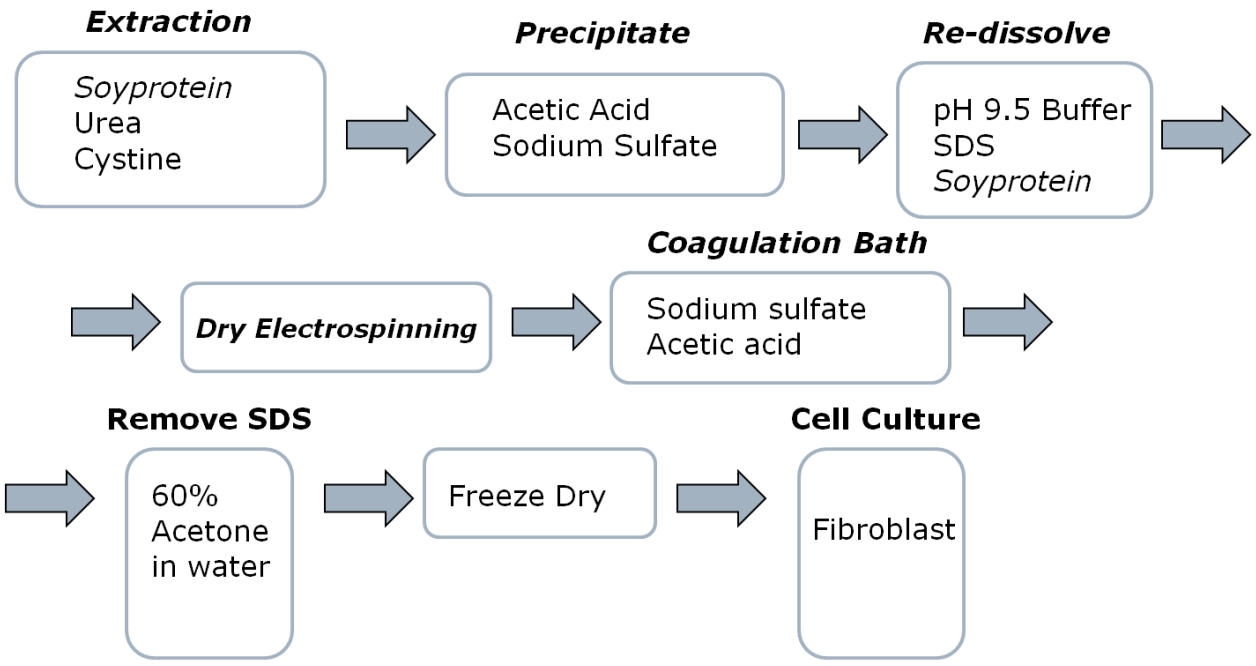

Figure 2 Fabrication of soyprotein 3D scaffold

Extracting Soyprotein

4.2. Extracting Soyprotein

Soyproteins was treated in 8 M urea under mild alkaline condition (pH 9.5) with 10% of cysteine (reducing agent) in order to obtain suitable molecular weight proteins that could be dissolved for electrospinning. After treating at 90 °C for 2 h, soluble proteins were collected by adjusting the pH of the solution to 3.5, and adding Na_2SO_4 (10% w/w, based on the weight of solution).

Properties of Extracted Soyprotein

4.3. Properties of Extracted Soyprotein

Extracted soyproteins were tested to determine their molecular weights. SDS-PAGE analysis was done to understand the effect of pre-treatment on molecular weights of the proteins. A

relationship was established between molecular weights, and solubility and spinability of the proteins.

Scaffolds Fabrication

4.4. Scaffolds Fabrication

2D zein scaffolds were prepared by electrospinning 25 wt% zein (Freeman Industries LLC, Tuckahoe, NY) in 70% v/v aqueous ethanol (EMD Chemicals Inc., Gibbstown, NJ) solution. Three dimensional zein scaffolds were prepared by electrospinning aqueous solution containing 25 wt% of zein and 25 wt% of SDS. Nine wt% (based on the weight of zein) of citric acid (EMD Chemicals Inc., Gibbstown, NJ) was added into both 2D and 3D spinning dopes for crosslinking. Three dimensional soyprotein scaffolds were prepared by electrospinning aqueous solution containing 32.5 wt% of extracted soyprotein and 17.5 wt% of SDS. Two dimensional soyprotein scaffolds were prepared by electrospinning aqueous solution with 32.5 wt% of extracted soyprotein and 17.5 wt% of SDS onto the positively charged collecting board covered by a layer of insulator. For both 2D and 3D soyprotein scaffold, no further cross-linking for soyprotein is needed. Different solvent systems for zein 2D and 3D scaffold were utilized since zein could not be dissolved in water.

All the electrospinning parameters, including the extrusion speed of 2ml h^{-1}, voltage of 42 kV and distance from the needle to the collecting board of 25 cm, were kept the same for all the samples. The needle was negatively charged and the collecting board was positively charged.

Morphologies and Structures of Scaffolds

4.5. Morphologies and Structures of Scaffolds

The 2D and 3D scaffolds were observed using scanning electron microscope (SEM, S3000N, Hitachi Inc. Schaumburg, IL) and a Nikon A1 confocal laser scanning microscope (CLSM, Nikon Inc., Melville, NY).

Specific Pore Volume

4.6. Specific Pore Volume

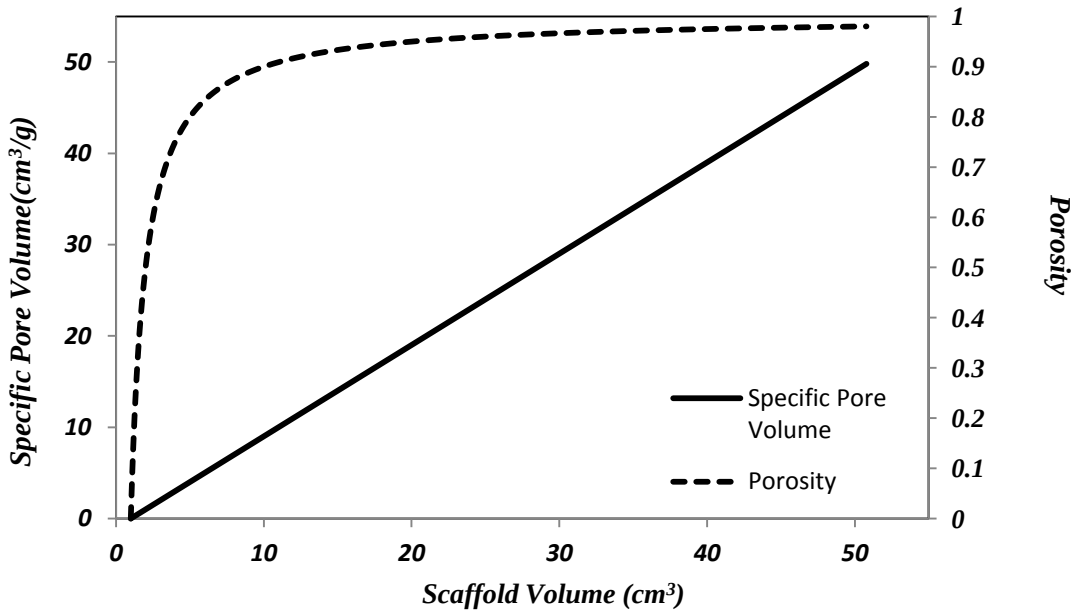

Figure 3 Influence of scaffold volume of unit mass on specific pore volume and porosity of scaffolds. The trend lines were drawn based on equation1 and 2 as shown below. Given that the mass of the scaffold was 1 g, and the density of the material was 1 g/cm^3.

Specific pore volume, namely volume of air in unit mass of scaffolds as shown in equation 1, was selected in this study to evaluate the fluffiness of the scaffolds.

$$V_{SP} = \frac{V_{pore}}{m_{scaffold}} = \frac{V_{scaffold}}{m_{scaffold}} - \frac{1}{\rho_{material}} \quad \text{Equation 1}$$

Whereas, V_{sp} is the specific pore volume, V_{pore} is the volume of air encompassed in the scaffolds, $m_{scaffold}$ is the mass of scaffolds, $V_{scaffold}$ is the volume of the scaffolds after precise measurement of the length, width and thickness of scaffolds, $\rho_{material}$ is the density of the scaffolds. In many reports regarding tissue engineering scaffolds, porosity, as calculated with Equation 2, was chosen to describe fluffiness of scaffolds.

$$\%P = \frac{V_{pore}}{V_{scaffold}} \times 100\% = \left(1 - \frac{m_{scaffold}}{V_{scaffold} \times \rho_{material}}\right) \times 100\% \quad \text{Equation 2}$$

Where, % P is the percent porosity. % P was not chosen here as a characteristic of scaffolds, because the porosity could not reflect change in fluffiness when the scaffolds have relatively high fluffiness. Assuming the mass of the electrospun scaffold is 1 g and the density of material is 1 g/cm^3, as fluffiness of the scaffolds increases, volume of pore per unit weight increases, as well as porosity and specific pore volume as shown in **Figure 3**. When the porosity is below 90, a small increment in volume could lead to obvious increase in porosity. On the contrast, if the porosity of scaffold is above 90, significant increase in scaffold volume could not result in obvious change in porosity. However, specific pore volume increases in a constant rate with the increase of scaffold pore volume, and therefore is a better characteristic of the fluffiness of the scaffolds. For instance, as the porosity increased from 80% to 89%, the porosity increased 9% while the scaffold volume per unit mass increased 200% as well as specific pore volume. Interestingly, as the porosity increased from 90% to 99%, the porosity increased 9% as before while the scaffold volume per unit mass increased 800% as well as specific pore volume. Therefore, porosity is competent to characterize porous structures with low degree of fluffiness, while specific pore volume is preferred here to describe 3D scaffolds with high fluffiness.

Water Stability

4.7. Water Stability

Soyprotein scaffolds were tested for water stability in PBS solutions. Stability studies were done at 37 °C using an incubator. At various time points (0 hours to 4 weeks), scaffolds was taken out of the solution and changes in the morphology was determined using electron microscopes.

Surface Resistivity:

4.8. Surface Resistivity:

Since the surface resistivity of ultra-fine fibers is very difficult to test, films contained same polymer to surfactant or salt ratio with relevant electrospun fibers were prepared to measure the surface resistivity. The films were casted onto Teflon coated plates and dried at 20 °C and 65% Relative Humidity. Surface resistivity was measured employing surface resistivity tester (Monroe Electronics Inc., Lyndonville, NY) according to ASTM D-257 standard.

Fiber Deposition Process

4.9. Fiber Deposition Process

A CCD camera with a long-working-distance lens was used in capturing the moment photographs of fiber deposition and scaffold formation. The time interval for each consequential photograph was 0.125 s.

In Vitro Cell Proliferation Study of Zein Scaffold

4.10. *In Vitro* Cell Proliferation Study of Zein Scaffold

4.10.1. Cell Attachment and Proliferation

NIH 3T3 mouse fibroblast cells (ATCC® CRL-1658™, Manassas, VA) were cultured to quantitatively estimate effects of 2D and 3D structures of zein scaffolds on cell attachment and proliferation. Cells were cultured in culture medium at 37 ℃ in a humidified 5% CO_2 atmosphere. Electrospun 2D and 3D zein scaffolds were first rinsed in 60 wt% acetone (BDH, West Chester, PA) aqueous solution containing 5 wt% of potassium chloride (Fisher Scientific, Fair Lawn, NJ) to remove SDS, washed in distilled water three times and then lyophilized. MTS assays were performed to quantitatively investigate cell viability at attachment and proliferation stages. Samples were prepared with same weight and then were subjected to sterilization at 120 ℃ for 1 h. After sterilization, the scaffolds were placed in 48-well culture plates (TPP® Techno Plastic Products, Switzerland). Fibroblast cells were seeded onto the scaffolds (1×10^6 cells ml^{-1}, 500 μl $well^{-1}$) and then cultured at 37 ℃ in a humidified 5% CO_2 atmosphere for different time intervals. At each time point, the samples were washed with PBS, placed in new 48-well plates containing 450 μl $well^{-1}$ 20% MTS reagent (CellTiter 96® Aqueous One Solution Cell Proliferation Assay, Promenade) in Dulbecco's modified Eagle's medium (DMEM) and incubated at 37 ℃ in a humidified 5% CO_2 atmosphere for 3 h. After incubation, 150 μl of the solution from each well was pipetted into a 96-well plate and the optical densities were measured at 490 nm using a UV/Vis multiplate spectrophotometer (Multiskan® Spectrum, Thermo Scientific). The MTS solution in DMEM without cells served as the blank.

4.10.2. Cell Penetration and Spreading:

To compare penetration ability of cells on 2D and 3D scaffolds, cells were stained by Phalloidin 633 solution (1: 200 Alexa Fluor 633 Phalloidin, Invitrogen, Grand Island, NY) and observed using a Nikon A1confocal laser scanning microscope (Nikon Inc., Melville, NY). Alexa Fluor 633 Phalloidin is a far red fluorescent dye that specifically bonds to F-actin in cells. This dye was selected since zein shows fluorescence across the full spectrum with weakest signal in the far red range. To observe the spreading behaviors and stereoscopic morphologies of cells in 2D and 3D scaffolds, cells were stained by Phalloidin 633 solution for F-actin and Hoechst 33342 solution (Invitrogen, Grand Island, NY) for the nuclei of cells.

In Vitro Stem Cell Adipogenic Differentiation Study of Soyprotein Scaffold

4.11. *In Vitro* Stem Cell Adipogenic Differentiation Study of Soyprotein Scaffold

4.11.1. Cell Seeding

Adipose-derived mesenchymal cells (ADMSCs ATCC® PCS-500-011™, Manassas, VA) were cultured to quantitatively estimate effects electrospun 2D and 3D soyprotein scaffolds and commercial 3D scaffolds (Biomerix 3D Scaffold ™) on cell attachment and proliferation. Electrospun 2D and 3D soyprotein scaffolds were first rinsed in 60 wt% acetone (BDH, West Chester, PA) aqueous solution containing 5 wt% of potassium chloride (Fisher Scientific, Fair Lawn, NJ) to remove SDS, washed in distilled water three times and then lyophilized. 2D and 3D soyprotein scaffolds was sterilized at 120 ℃ for 1 h in an autoclave. Commercial 3D scaffolds were immersed in 70% aqueous ethanol over night for sterilization. After sterilization, all the scaffolds were rinsed in PBS before cell culture. For cell seeding, each scaffold weight 10mg was prepared. All scaffolds were placed in 48-well culture plates (TPP® Techno Plastic Products, Switzerland). ADMSCs were seeded onto the scaffolds in a density of 3×10^5 cells ml^{-}

^{1} and 500 μl well^{-1} , and then cultured in Dulbecco's modified Eagle's medium (DMEM, with 10% FBS, 1% antibiotic solution) at 37 ℃ in a humidified 5% CO_2 atmosphere.

4.11.2. Cell Attachment and Proliferation

MTS assays were performed to quantitatively investigate cell viability at attachment and proliferation stages. At each time point (4 hours, 5 days, 10 days and 15 days), the samples were washed with PBS, placed in new 48-well plates containing 450 μl well^{-1} 20% MTS reagent (CellTiter 96® Aqueous One Solution Cell Proliferation Assay, Promenade) in Dulbecco's modified Eagle's medium (DMEM) and incubated at 37 ℃ in a humidified 5% CO_2 atmosphere for 3 h. After incubation, 150 μl of the solution from each well was pipetted into a 96-well plate and the optical densities were measured at 490 nm using a UV/Vis multiplate spectrophotometer (Multiskan® Spectrum, Thermo Scientific). The MTS solution in DMEM without cells served as the blank. For each point of data, at least four samples were tested.

4.11.3. Adipogenic Differentiation of ADSCs

ADSCs were seeded onto all scaffolds (each scaffold weight 10mg) placed in 48-well culture plates at a density of 3×10^5 cells ml^{-1} and 500 μl well^{-1} in DMEM (with 10% FBS, 1% antibiotic solution) at 37 ℃ in a humidified 5% CO^2 atmosphere, and allowed to adhere for 24 h. After 24 h, DMEM was then replaced by adipogenic differentiation medium (Adipocyte Differentiation Toolkit, ATCC® PCS-500-050™). Adipogenic differentiation media was renewed every 3 or 4 days.

4.11.4. Adipogenic Differentiation Evaluation

Cell differentiation was evaluated by staining with Oil red O (Sigma, St. Louis, MO, USA). ADSCs was cultured in adipogenic medium for different time interval (5 days, 10 days and 15

days), and then fixed in a 10% solution of formaldehyde (Sigma, St. Louis, MO) in PBS at least 1 h, and then was washed with 60% isopropanol (Sigma, St. Louis, MO, USA), and stained with Oil red O solution (in 60% isopropanol) for 10 min followed by repeated washing with water, and destained in 100% isopropanol for 15 min. The optical density (OD) of the solution was measured at 500nm using a UV/Vis multiplate spectrophotometer (Multiskan® Spectrum, Thermo Scientific). For each point of data, at least four samples were tested.

4.11.5. Analysis of Newly Formed Tissues:

At different time interval after seeding and differentiation, newly formed tissues were retrieved and analyzed histological. Frozen sections were constructed by slicing the samples into 50 μm sections using a cryostat, and then embedding on cover slips. The slides were stained with Oil red O and examined under both light microscope (Olympus BX60, IX70 Olympus Optical Co., Tokyo, Japan).

4.11.6. Cell Penetration and Spreading:

To compare penetration ability of cells on 2D and 3D scaffolds, and commercial 3D scaffolds, cells were stained by Hoechst 33342 solution (Invitrogen, Grand Island, NY), and observed using a Nikon A1confocal laser scanning microscope (Nikon Inc., Melville, NY). Hoechst 33342 solution (Invitrogen, Grand Island, NY) is blue dye for nuclei of cells.

Statistical Analyses or Qualitative Analyses

4.12. Statistical Analyses or Qualitative Analyses

One-way analysis of variance with Tukey's pairwise multiple comparisons was employed to analyze the data. The confidence interval was set at 95% and a P value less than 0.05 was

considered to be a statistically significant difference. In the results, data labeled with the same symbols were **not** significantly different from each other.

CHAPTER 5: RESULTS AND DISCUSSION

Extraction of Spinnable Soyproteins

5.1. Extraction of Spinnable Soyproteins

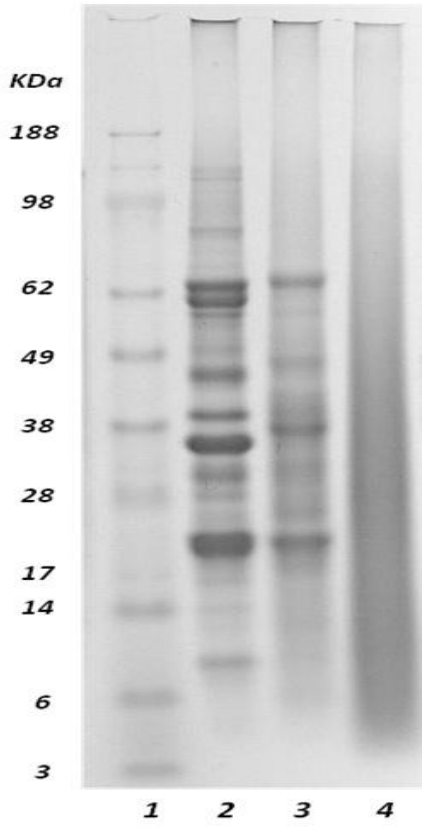

Figure 4 SDS-PAGE of soy protein. Lane 1 is standard protein marker, lane 2 is original soy protein, lane 3 is soy protein extracted with cysteine and urea, lane 4 is NaOH extracted soy protein.

Soyproteins is a crosslinked protein and the presence of cysteine crosslinkages makes it very difficult to dissolve soyproteins in water or common solvents. Soyproteins was treated in 8 M urea under mild alkaline condition with 10% of cysteine (reducing agent) in order to obtain

proteins with suitable molecular weight that could be dissolved for electrospinning. After treating at 70 °C for 24 h, soluble proteins were collected.

SDS-PAGE results showed that the molecular weights of cysteine extracted soyproteins were a little bit lower while the main bands were kept, if compared to that before treatment. Lane 1, 2 and 3 were untreated soy protein, cysteine extracted soy protein and soy protein treated with NaOH. It could be seen that major bands (20 kDa, 37 kDa and 63 kDa) of soy protein remained in the extracted sample, while no obvious bands could be found in the NaOH treated sample. Cysteine could break the disulfide bonds of soyprotein without harm the main polymer chain too much. The solubility and spinability of untreated soy protein, cysteine extracted soy protein and soy protein treated with NaOH was shown in **Figure 5** and **Figure 6**.

Solubility and Spinnability of the Soyproteins

5.2. Solubility and Spinnability of the Soyproteins

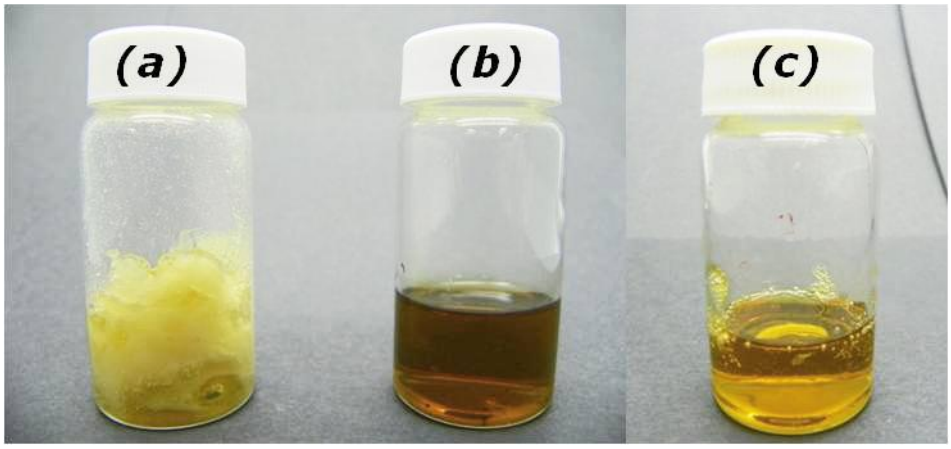

Figure 5 Solubility of (a) untreated soy protein, (b) cysteine extracted soy protein and (c) soy protein treated with NaOH. All solution contains 32.5 wt% of soyprotein and 17.5 wt% of SDS.

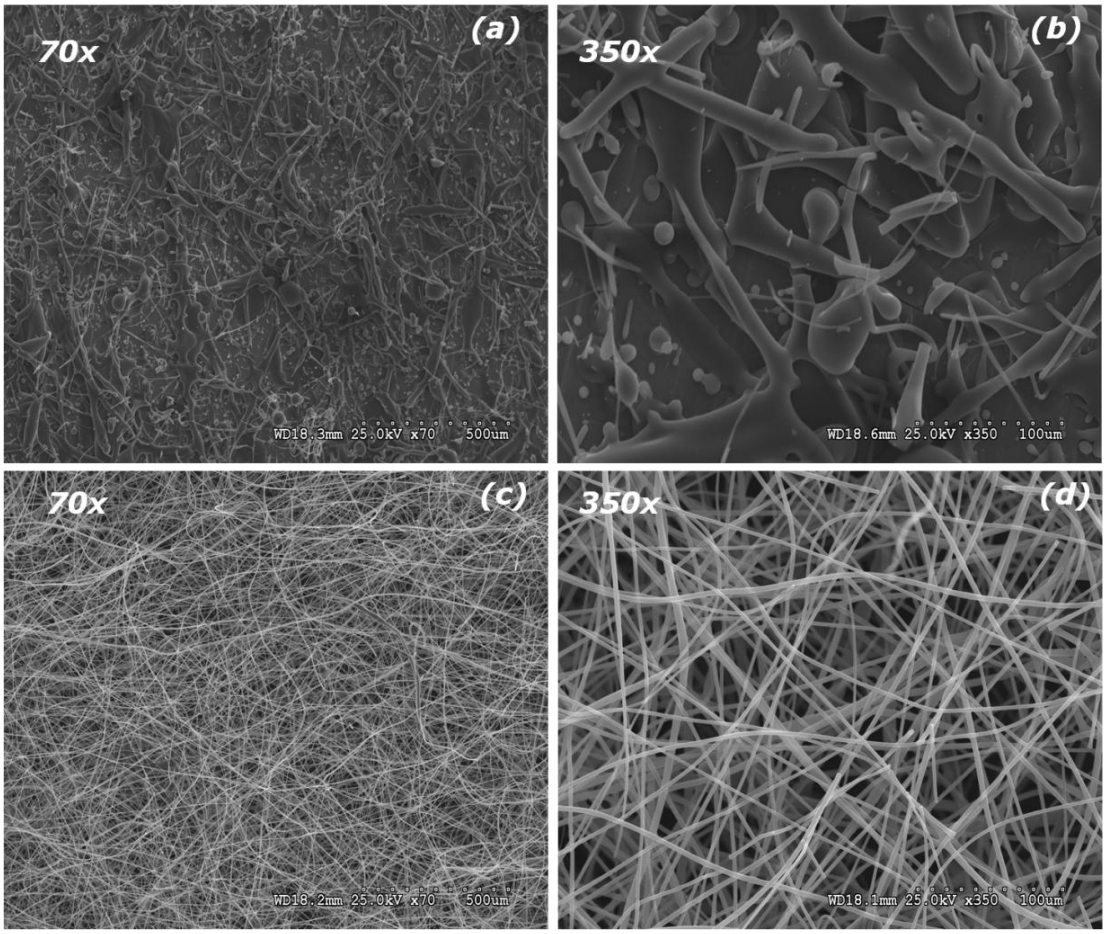

Figure 6 Electrospining result of (a) (b) soy protein treated with NaOH and (c) (d) cysteine extracted soyprotein. All electrospining solution contains 32.5 wt% of soyprotein and 17.5 wt% of SDS. (a) (c) SEM top view images at magnifications of 70 x, (a) (c) SEM top view images at magnifications of 350 x.

It can be found that untreated soy protein cannot be dissolve in the spinning solution, because soyprotein is a globular protein, which contains many intermolecular and intramolecular disulfide bond crosslinkages which are very stable in most common organic solvents that are suitable for electrospinning. Soyproteins treated with NaOH and extracted by cysteine can both be dissolved in the electrospining solution with 17.5 wt% of SDS.

However, only soyprotein extracted by cysteine can be electrospun into ultrafine fibers. When dissolve SPI with strong alkali condition, it will hydrolyze and break down SPI molecules chains into small fractions which are much easier to dissolve. This degradation process will also decrease the spinning ability of the solution, because the entanglement of the small fractions is also quite low. SPI dissolved in alkaline solution could be used for electrospining only by blending SPI with other polymers, such as PEO or zein. As mentioned above, the blending process may change the biocapability and biodegradability of SPI. Moreover, the water stability of the hydrolyzed soy proteins scaffold may also problematic, further crosslinking may be needed for many biomedical applications. Cross-linking has been used as alternatives to polymer blending. However, most cross-linking agents are toxic and expensive, and therefore cross-linking may decrease the biocompatibility and increase cytotoxicity of natural protein materials.

Morphologies and Structures of Scaffolds

5.3. Morphologies and Structures of Scaffolds

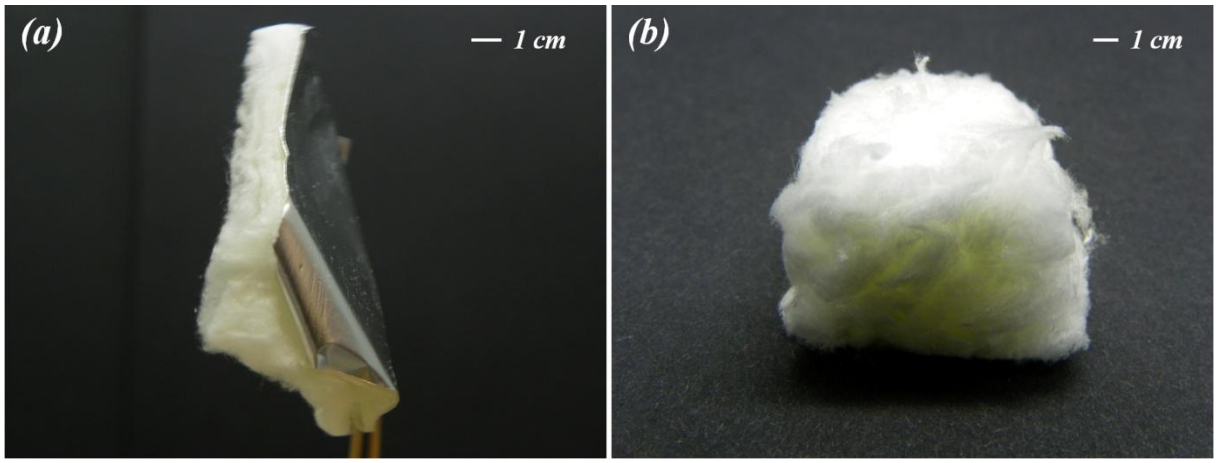

Figure 7 Digital photos of 3D zein electrospun scaffolds a) as-spun scaffold with aluminum foil; b) scaffold ready for wash and use for cell culture.

As seen from the digital images in **Figure 7** and **Figure 8a**, 3D (**Figure 7** and **Figure 8a (left)**) scaffolds with porosity of 99.6% has remarkably higher fluffiness than 2D (**Figure 8a (right)**) scaffold with porosity of 79.4% of the same weight. In scanning electron microscope (SEM) images of the 2D zein scaffold, the front views (**Figure 8c and c'**) demonstrated that fibers packed closely, and in the side views (**Figure 8e and e'**), tightly stacked sheets were observed. From both views, only a few pores larger than 10 μm could be found. However, the fibers in 3D zein scaffold packed loosely and multiple pores with sizes larger than 100 μm could be seen on the top surface (**Figure 8d and d'**) and side (**Figure 8 f and f'**). As reported, migration and penetration of cells into the interior of scaffolds necessitated introduction of pores larger than 100 μm into the structures. [66] Thus, 3D scaffolds developed in this study would be preferred in cell culture due to the larger space available for cells to attach and infiltrate.

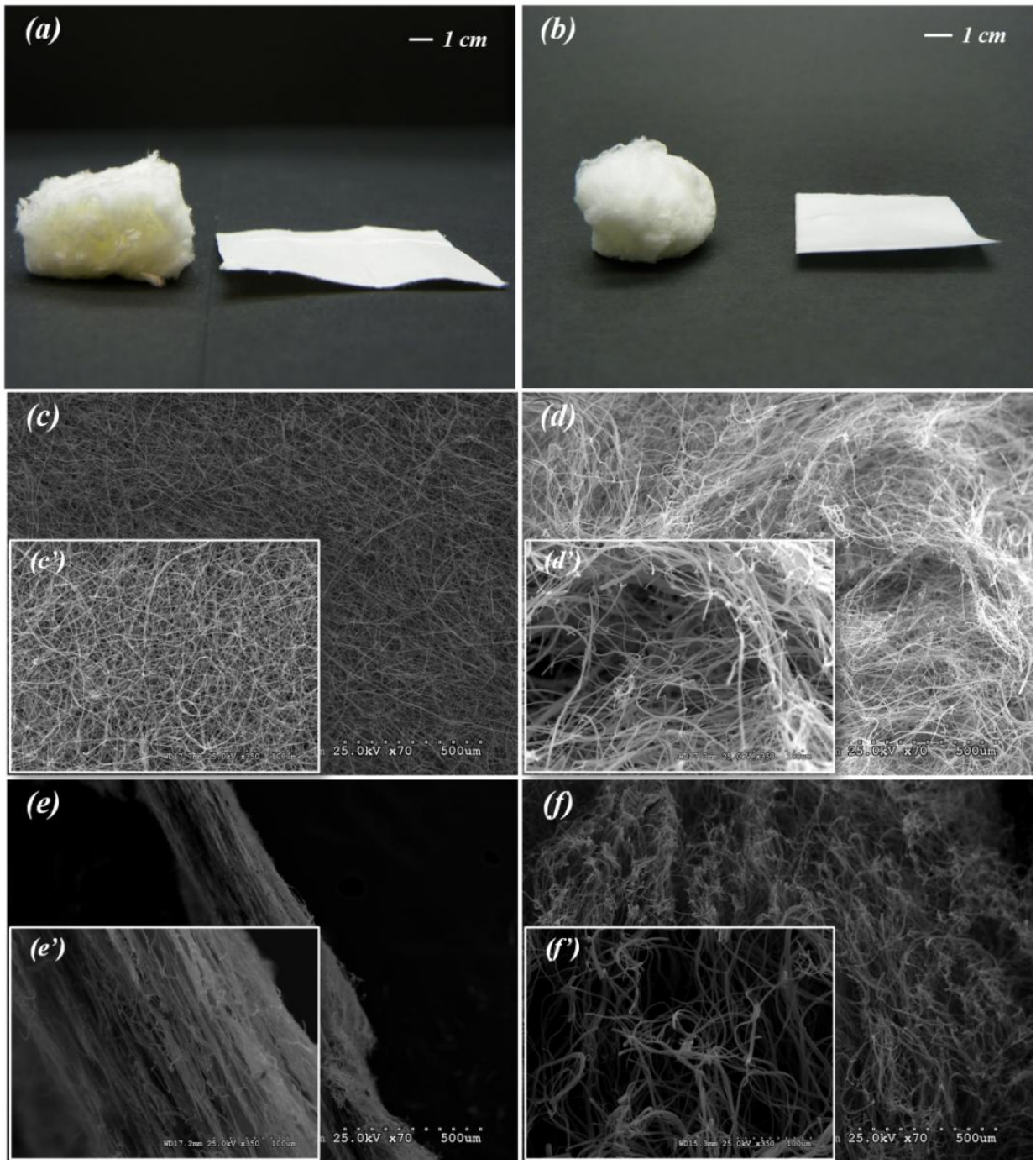

Figure 8. Morphological comparisons between 2D and 3D electrospun zein and PEG scaffolds. a) Digital photo of 3D (left) and 2D (right) zein electrospun scaffolds with the same weight; b) Digital photo of 3D (left) and 2D (right) PEG electrospun scaffolds with the same weight; c) and d) SEM top view images at magnifications of 70x (c) and 350x (c') of 2D zein electrospun

scaffold and 70x (d) and 350x (d') of 3D zein electrospun scaffold; e) and f) SEM side view images at magnifications of 70x (e) and 350x (e') of 2D zein electrospun scaffold and 70x (f) and 350x (f') of 3D zein electrospun scaffold.

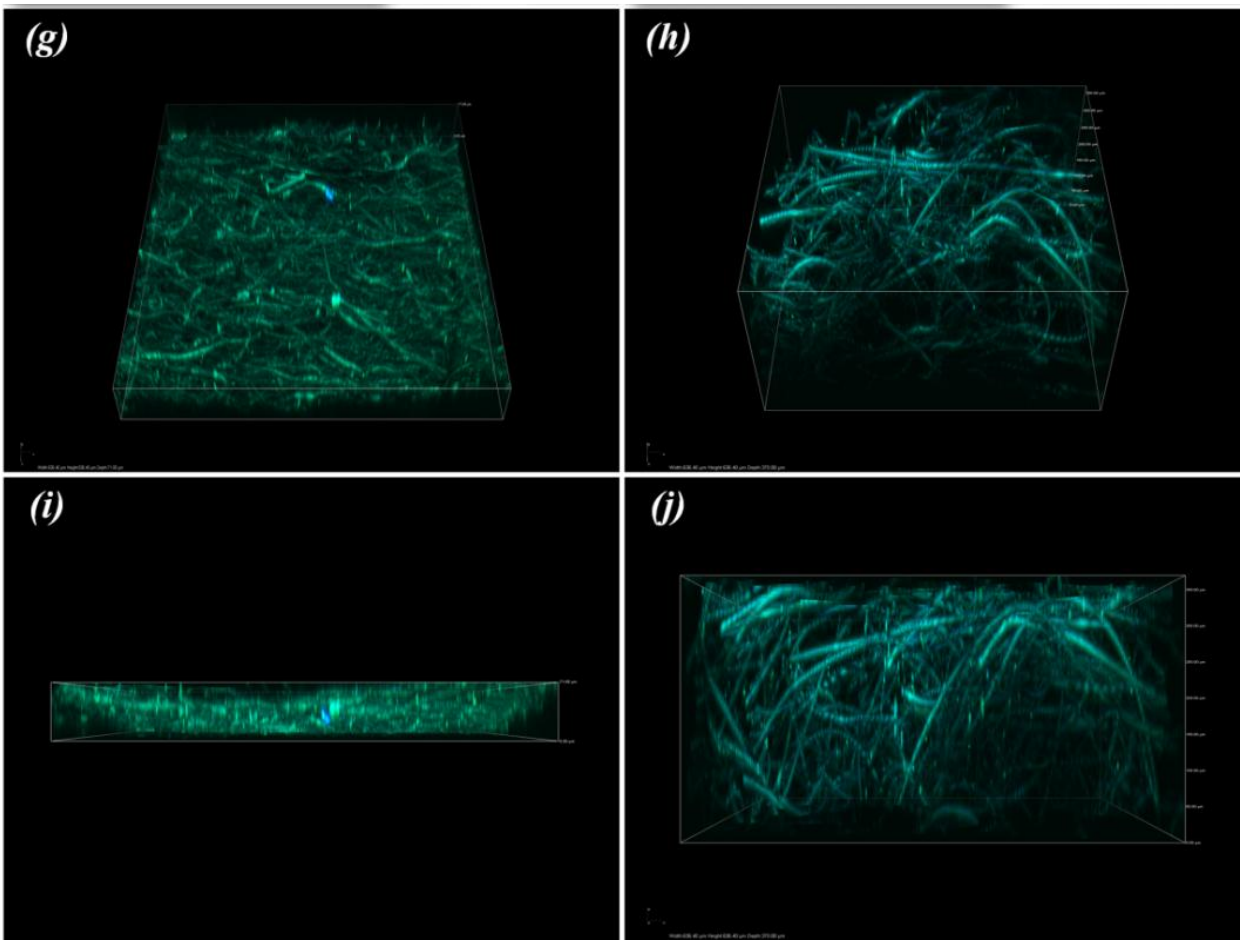

Figure 9. g) and h) CLSM 45 degree view images at magnification of 100x of 2D (g) and 3D (h) zein scaffolds; i) and j) CLSM side view image at magnification of 100x of 2D (i) and 3D (j) zein electrospun scaffolds.

Furthermore, three-dimensionally randomly oriented fibers in all directions including the thickness direction rendered the 3D zein scaffold structurally more similar to that in the native ECMs. As seen from the SEM (**Figure 8 c-f**) and confocal laser scanning microscope (CLSM) images (**Figure 9 g-j**), random arrangement and haphazard orientation of fibers could be

observed in the 3D zein scaffold, while regularly piled fibrous mats in the 2D zein scaffold indicated few fibers oriented in the thickness direction. Therefore, compared to that on 2D scaffolds with highly stacked structures, cells cultured on 3D scaffolds would develop into more ellipsoidal and stereoscopic types.

To verify the potential of applying this novel 3D electrospinning method to materials other than proteins, polyethylene glycol (PEG) was 3D electrospun as well. The 3D and 2D PEG electrospun scaffolds were shown in **Figure 8 b** left and right, respectively. The 3D PEG scaffold was also featured for the high pore content and loose structure as 3D zein scaffold, whereas the 2D PEG scaffold with tight structure, which resembled 2D zein scaffold. Similarly result of soyprotein 3D scaffold (**Figure 8** and **Figure 10 (b)**) and 2D (**Figure 10 (a)**) scaffold could be observed.

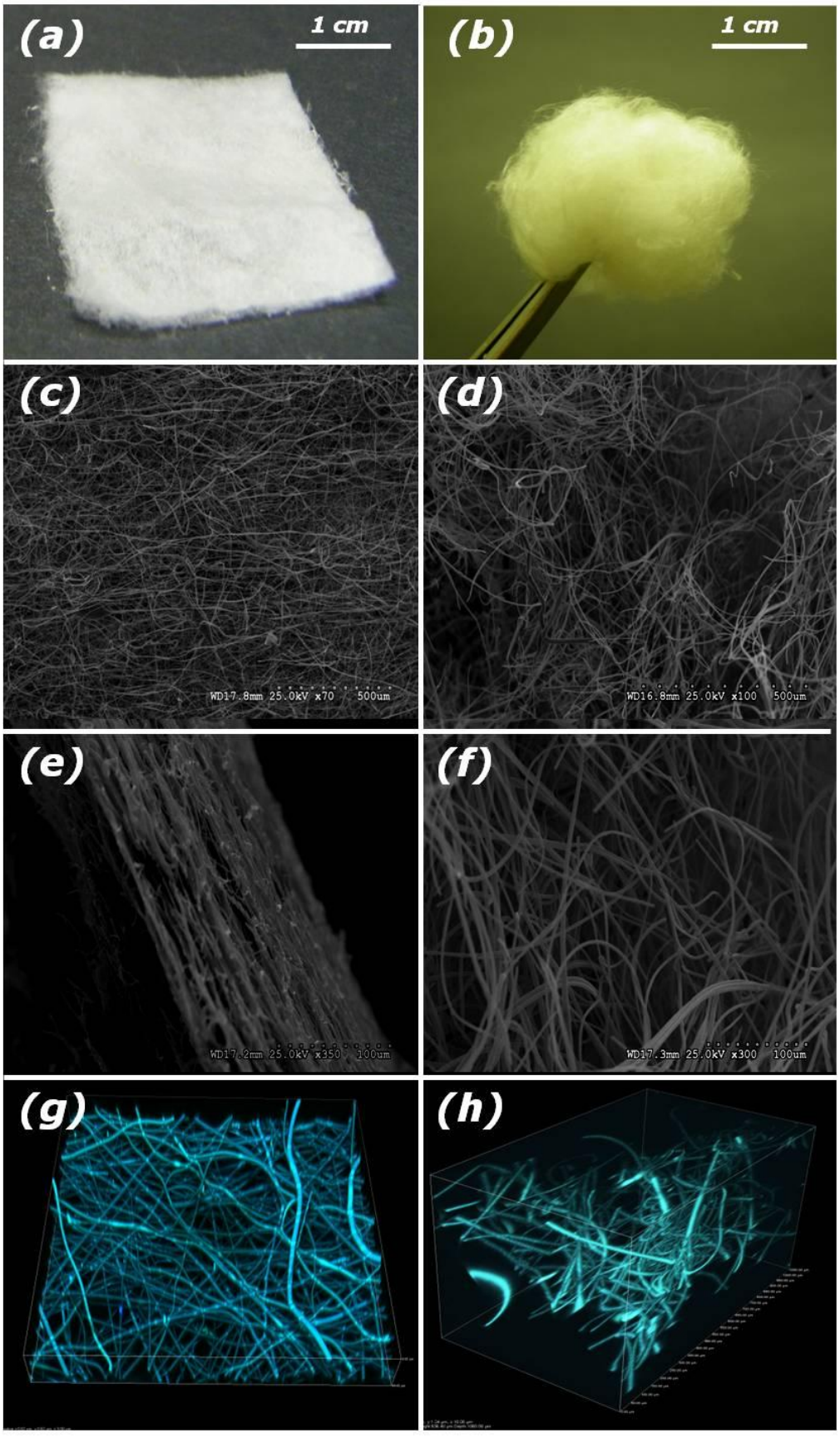
(a)
1 cm
(b)
1 cm
(c)
WD17.8mm 25.0kV x70 500um
(d)
WD16.8mm 25.0kV x100 500um
(e)
WD17.2mm 25.0kV x350 100um
(f)
WD17.3mm 25.0kV x300 100um
(g)
(h)

Figure 10. Morphology comparisons between 2D and 3D electrospun soyprotein scaffolds. a) Digital photo of 2D soyprotein electrospun scaffolds; b) Digital photo of 3D soyprotein electrospun scaffolds; c) and d) SEM top view images at magnifications of 70x of 2D soyprotein electrospun scaffold and of 3D soyprotein electrospun scaffold; e) and f) SEM side view images at magnifications of 70x of 2D soyprotein electrospun scaffold and 70x of 3D soyprotein electrospun scaffold; g) and h) CLSM 45 degree view images at magnification of 100x of 2D (g) and 3D (h) soyprotein scaffolds.

Proposed Mechanism

5.4. Proposed Mechanism

Difference in 2D and 3D electrospinning structures was assumed to be induced by different transient electrical force when fibers hit collecting board. It is proposed that sufficiently high surface electrical conductivity or low electrical resistivity of polymer is the premise for formation of 3D scaffolds. In both conventional and 3D electrospinning, at the beginning, the liquid droplet acquired negative charges and then was elongated into fibers. As shown in **Figure 11**, both conventional (**Figure 11a and c**) and 3D (**Figure 11b and d**) electrospun fibers with large amount of surface negative charges flew towards the collecting board perpendicularly. For conventional electrospinning, few of electrons transferred to the collector at the moment the fiber ends hit the collector, owing to high surface resistivity of the fibers. The fibers with large amount of remaining electrons were strongly attracted by the positive collector. As a consequence, conventional 2D electrospun scaffolds with fibers oriented parallel to the collecting board were obtained.

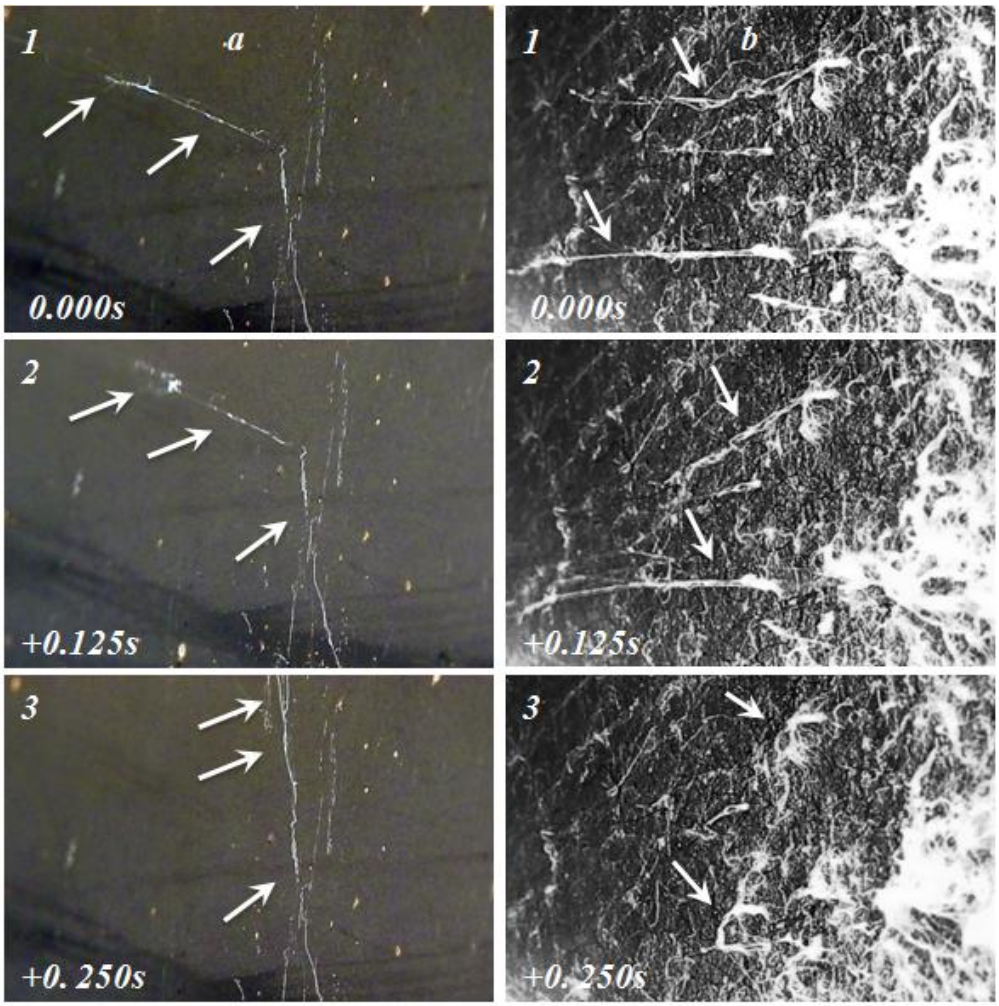
1
a
0.000s
2
+0.125s
3
+0. 250s
1
b
0.000s
2
+0.125s
3
+0. 250s

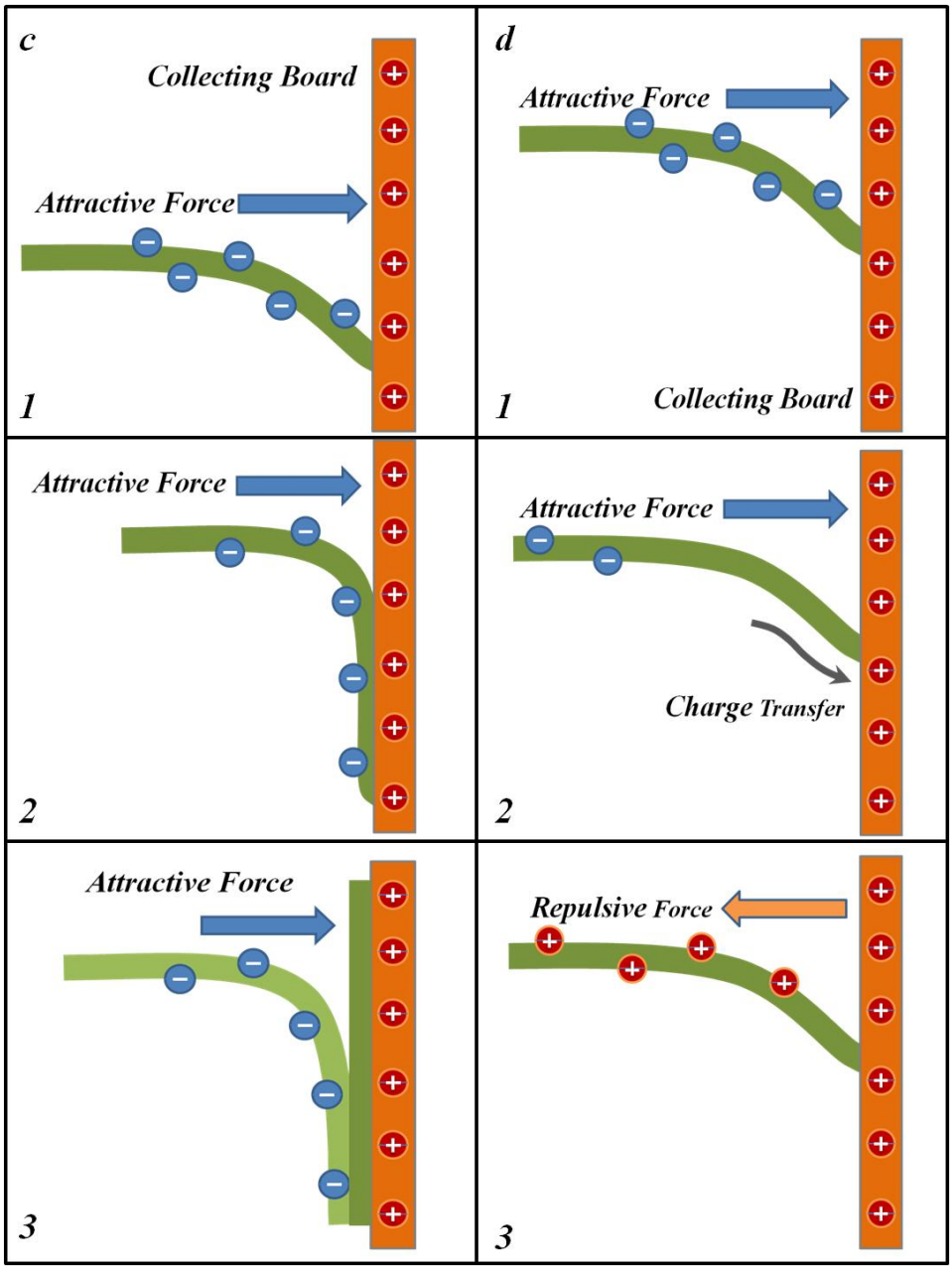

Figure 11. a) and b) Continuous photography of deposition processes of PEG fibers in 2D (a) electrospinning and 3D (b) electrospinning with time interval of 0.125 s between two sequential photographs. White objects in the images were PEG fibrous bulks. c) and d) Schematic diagram of deposition of fibers in 2D (c) and 3D electrospinning (d) processes. The needle was negatively charged and the collecting board was positively charged. Orange: the collecting board; dark green: fibers deposited on the collecting board at the beginning; light green: fibers deposited on

the collecting board afterwards; blue arrow: attractive force; orange arrow: repulsive force; gray arrow: the direction of electron transfer; blue circle: negative charge; red circle: positive charge.

Contrastively, for 3D electrospinning, low surface resistivity of fiber led to high transferability of charges from the fiber surface to the collector. When the fibers stroke the collector, surface static electricity could transfer to the board in a much faster manner, thus less negative static electricity was left on the fibers, and decreased attraction between fibers and collector. In some cases, the near portion of the fibers could even carry positive charges and could be repulsed by the collector, while rear end of the fiber was still attracted and moved towards the board. As a consequence, fibers were collected onto the board in multiple orientations and resulted in forming loose and fluffy 3D scaffolds.

Mechanism Validation

5.5. Mechanism Validation

A power function was used to simulate the relationship between the specific pore volume of electrospun scaffolds and corresponding polymer surface resistivity. As shown in **Figure 12a**, the residual standard error of the model is 0.613, which is a reasonable number to indicate that the data could be well described by power function and suggest that there is a strong quantitative relationship between the specific pore volume and surface resistivity. Hence, it verifies the theory proposed above. The power function was constructed as:

$$y = ax^b \qquad \text{Equation 3}$$

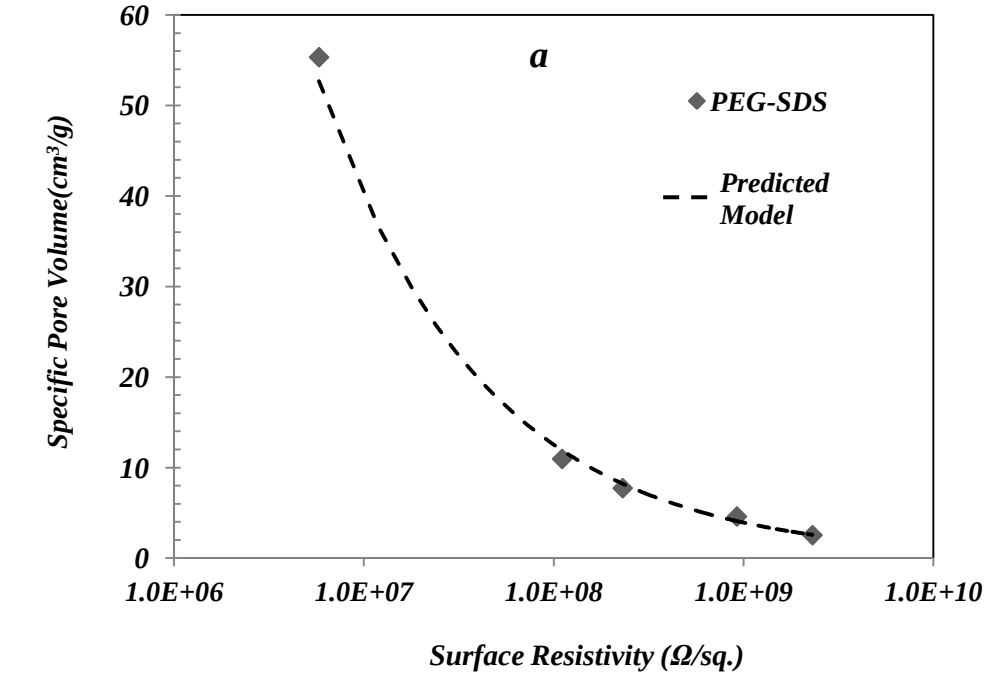

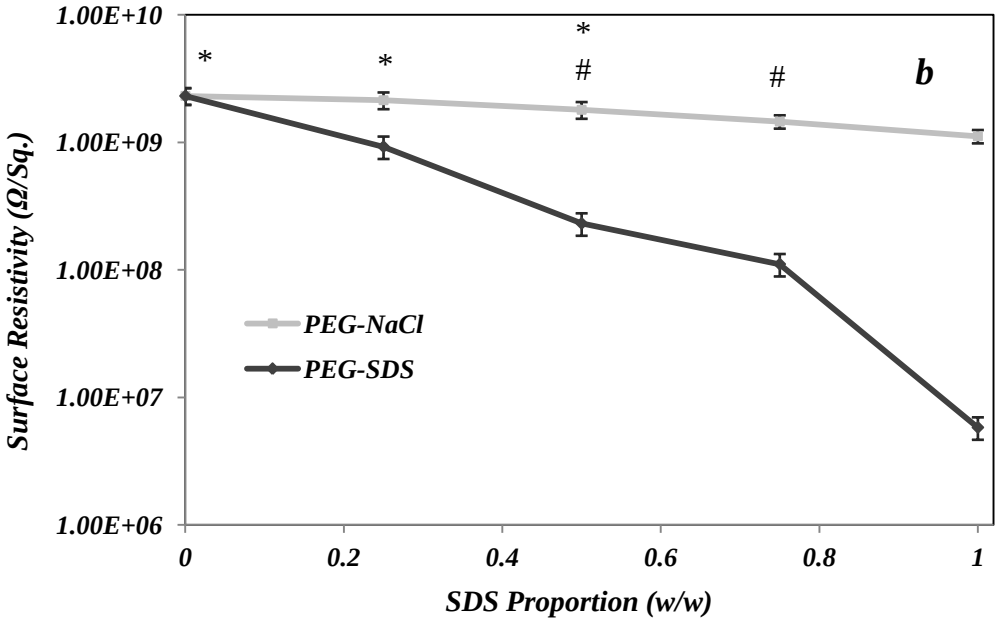

Figure 12. a) Relationship between specific pore volume of electrospun scaffolds and surface resistivity. The dash line shows the simulated relation using power function; b) Effect of sodium

dodecyl sulfate (SDS) and NaCl on surface resistivity of PEG films based on the proportions of SDS to polymer. The molar concentration of NaCl was the same as SDS at each point.

Where y represented specific pore volume, x represented surface resistivity, a and b were coefficients varied with the type of materials. Here, for PEG, a equaled to 2.208E+05 and b equaled to -0.5325. The specific pore volume decreased exponentially as surface resistivity increased. As surface resistivity decreased from 10^9 to 10^6 Ω/Sq., the macro structure of PEG scaffolds converted from 3D to 2D, and the specific pore volume decreased by about 20 times. It could be inferred that the increased surface conductivity increased fluffiness of scaffolds exponentially.

It was found that surface resistivity of polymer decreased with increasing SDS proportion. As shown in **Figure 12a**, surface resistivity of PEG decreased as SDS content increased. Surface resistivity of pure PEG was higher than 10^9 Ω/Sq.. When the weight ratio of SDS to PEG was increased to 1:1, surface resistivity was reduced considerably to 10^6 Ω/Sq.. However, when NaCl was added into the polymer, the surface resistivity did not decrease as substantially as the same mole of SDS was added. This is because when water evaporated, SDS mainly distributed on the surface of polymer while NaCl may distribute more evenly in the polymer. [67] The sulfate groups of SDS that concentrated on the surface of fiber oriented towards the outside, and could induce formation of a surface water layer on the fibers. In the surface water layer of PEG fibers, free movement of dissociable sodium ions from SDS effectively decreased surface resistivity of PEG electrospun fibers. Whereas the evenly distributed NaCl would only decrease the volume resistivity but could not effectively decrease surface resistivity of fibers. In summary, by adding

SDS, the polymer was converted from insulator to semi-conductor, the capability of transferring static electricity of the fiber has been tremendously increased, and correspondingly increased the fluffiness of scaffolds.

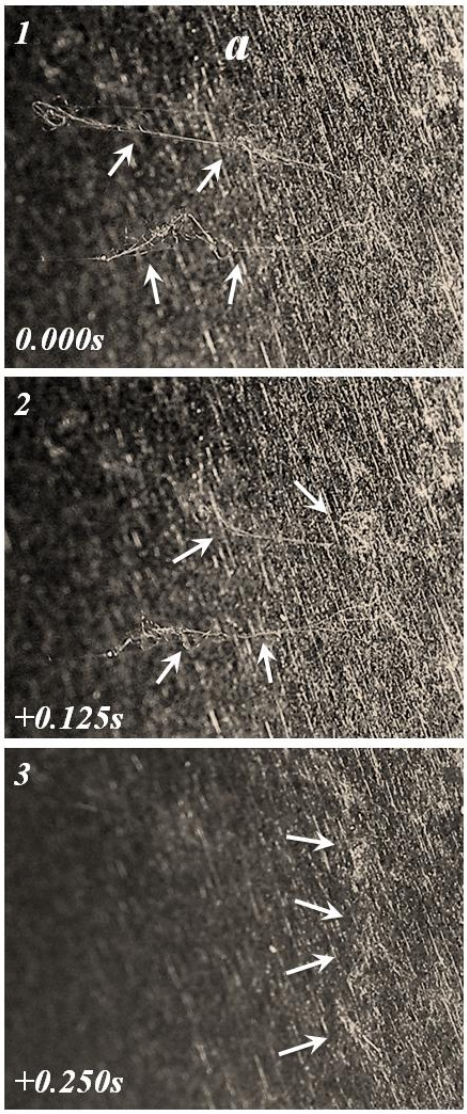

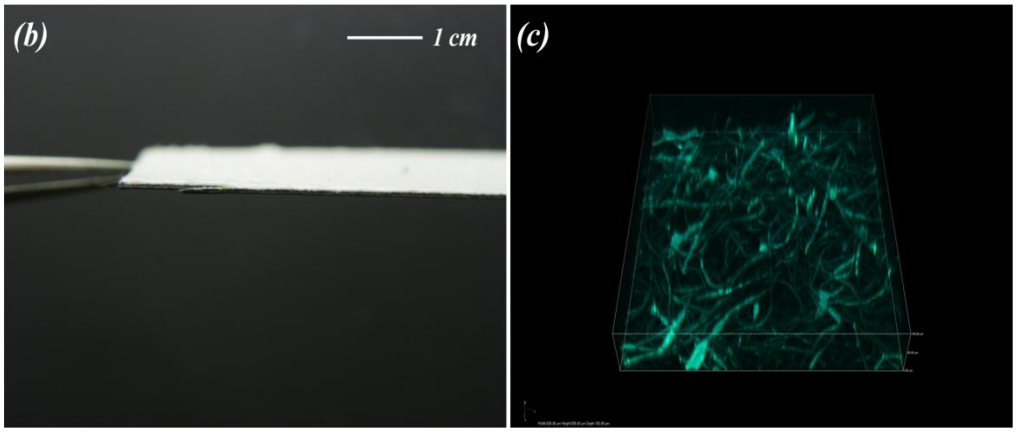

Figure 13. a) Deposition process of zein onto the insulator covered collector with time interval of 0.125 s between two sequential photographs. The spinning dope consisted of 25 wt% zein and 25 wt% SDS. b) Digital photo of the as-spun zein scaffold produced by electrospinning spinning dope with 25 wt% zein and 25 wt% SDS. c) CLSM 45 degree view images at magnification of 100x of the above as-spun zein scaffold.

To further investigate the effect of electron transference on formation of 3D architectures, solution with 25 wt% of zein and 25 wt% of SDS was electrospun onto the positively charged collecting board covered by a layer of insulator. Delivery of electrons was interrupted though positive potential still existed. Zein fibers with electrons on the surface were attracted by the positive collector and then hit the board vertically as shown in **Figure 13a**. However, the electrons could not be transferred onto the collecting board and thus remained on the fibers. The highly negatively charged fibers attached onto the insulator tightly owing to the strong electrical attraction, and consequently a traditional 2D electrospinning scaffold (**Figure 13 b** and **c**) was formed. As a conclusion, the proposed theory that rapid delivery of electrons on the fibers was the crucial factor for formation of 3D architectures had high validity.

Water Stability Test

5.6. Water Stability Test

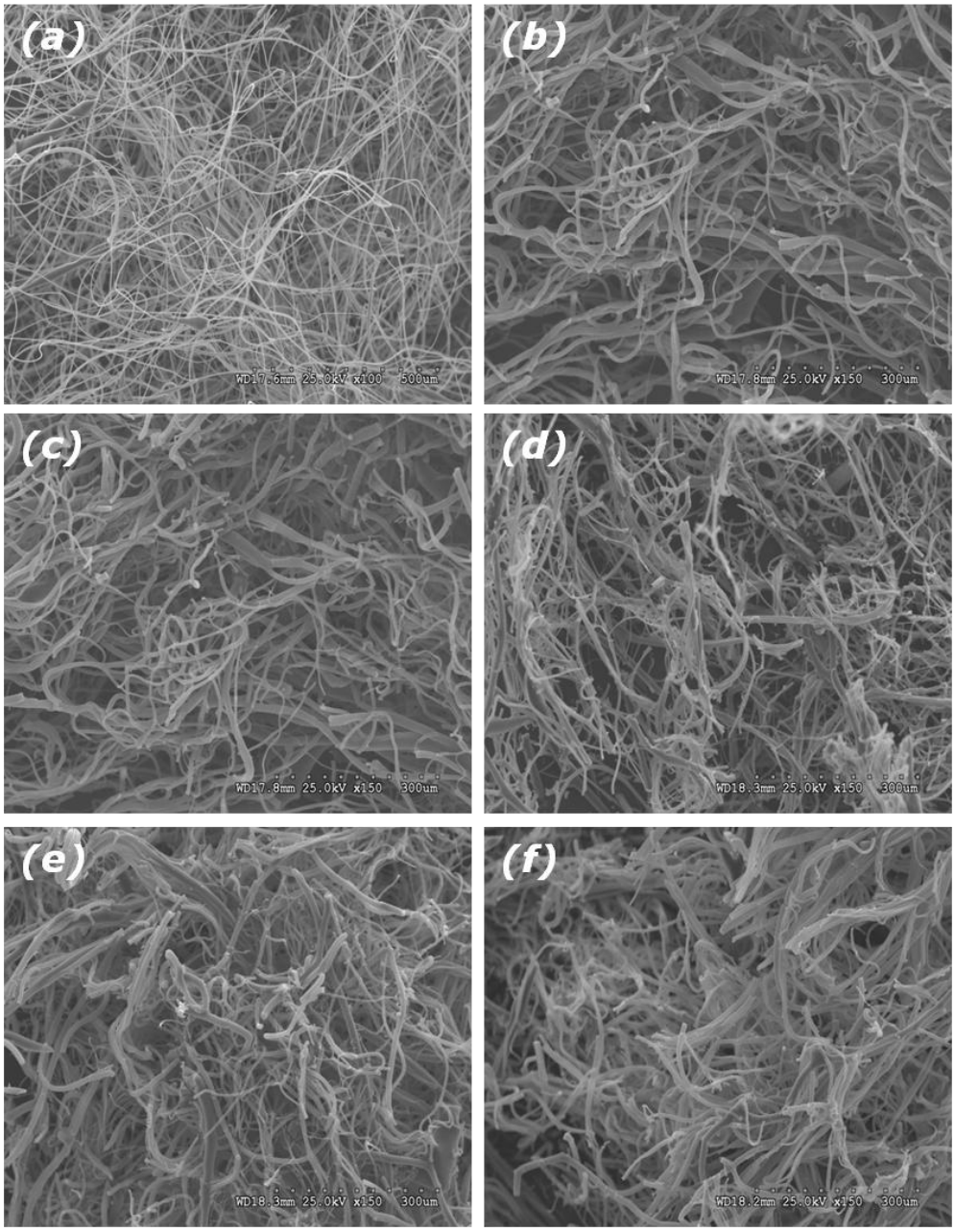

Figure 14 (a) as-spun soyprotein fibers, (b) to (f) soyprotein fibers immersed in PBS at 37 ℃ for (b) 3 days, (c) 1week, (d) 2 weeks, (e) 3 weeks and (f) 4 weeks.

It is found that after soyprotein fibers immersed in PBS at 37 ℃ for up to 4 weeks, the scaffold still can main its fibrous structure, thought swelling was occurred, and the diameter of the fibers was increased. Thus, for both 2D and 3D soyprotein scaffold, no further cross-linking is needed for future biomedical applications. Due to most cross-linking agents are toxic and expensive, avoiding cross-linking may help maintaining the biocompatibility and decrease possible cytotoxicity for soyprotein.

In vitro Cell Proliferation Study of Zein Scaffold

5.7. *In vitro* Cell Proliferation Study of Zein Scaffold

In vitro cell culture study results showed the 3D scaffolds were remarkably better than 2D scaffolds to support cell growth. As shown in **Figure 15 a**, noteworthy increase in attachment and proliferation rates of fibroblast cells were found in 3D scaffolds. The amount of cells attached on 3D scaffolds was 114% higher than that on 2D scaffolds. A plateau of methanethiosulfonate (MTS) results was reached 5 days after cell cultured on 3D scaffolds and the proliferation of cells increased by 439%. For 2D scaffolds, the plateau of MTS result was found 3 days after seeding, and the proliferation of cells increased by 181%. Most currently reported 3D scaffolds only showed 1.5- to 2.5-fold of improvement on the comparison of 3D scaffolds with their 2D counterparts after 5 to 7 days of cell culture. The results were consistent with the observation in the CLSM montage images in **Figure 15 b** and **c**. After 72 hours of cell culture, cells were found at least 120 μm beneath the surface of 3D scaffold, while cells could not be found 20-30 μm under the surface of 2D scaffold. The tight packing of fibers in the 2D scaffolds restricted penetration of cells vertically, while the multiple pores with much larger size

and significantly higher porosity of 3D scaffolds facilitated migration and penetration of cells into the interior of the structures.

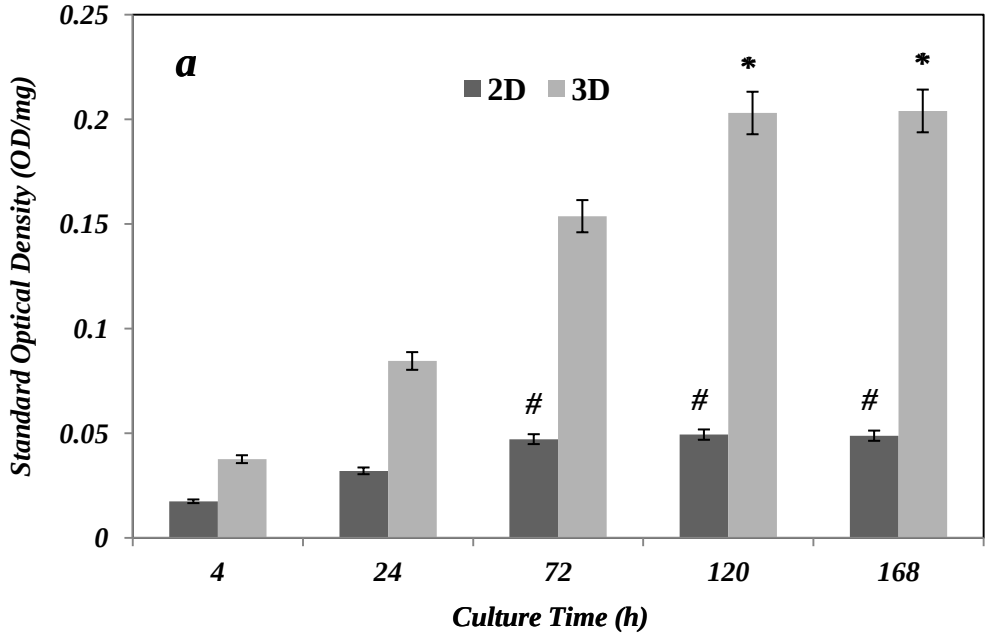

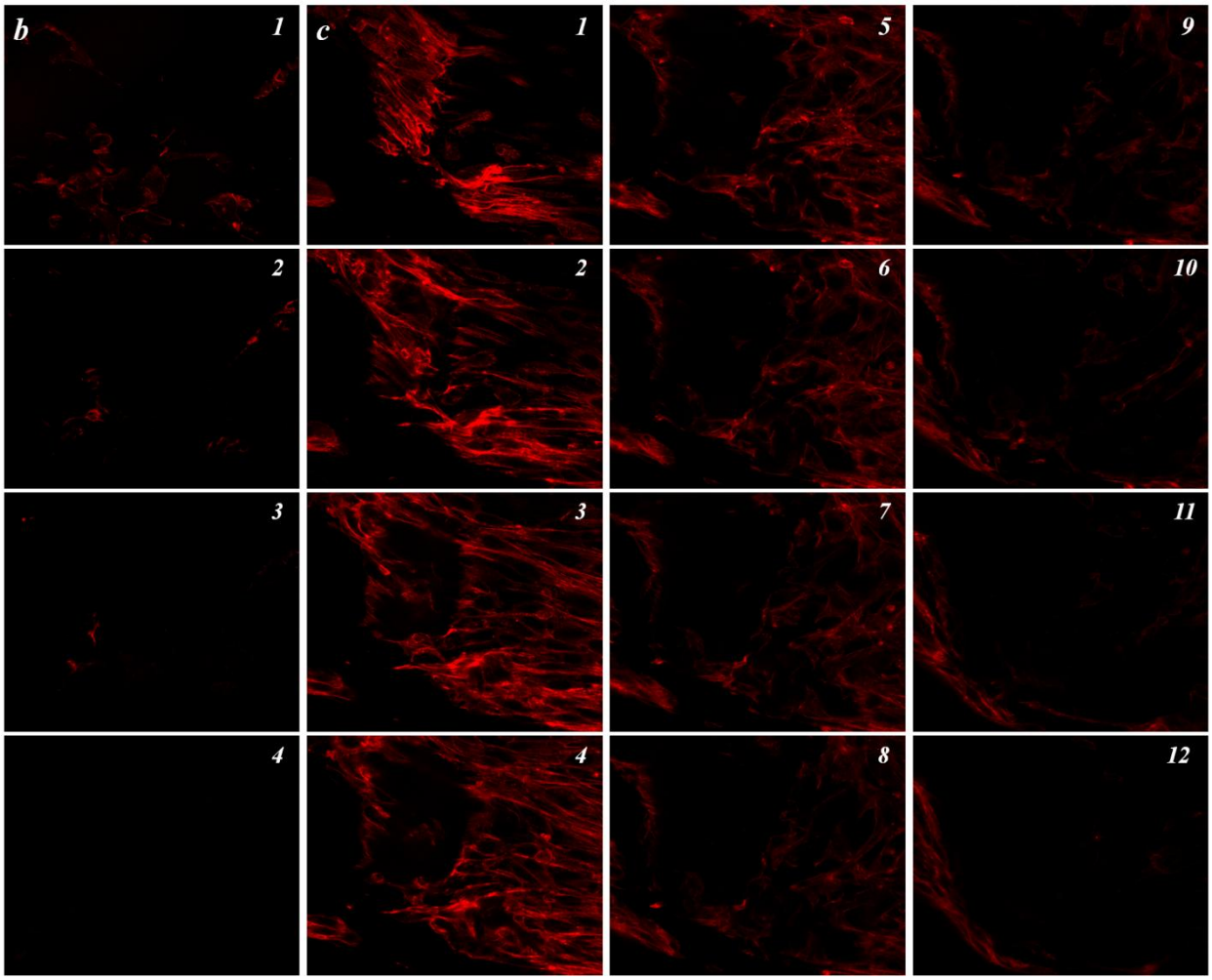
b
1
2
3
4
c
1
2
3
4
5
6
7
8
9
10
11
12

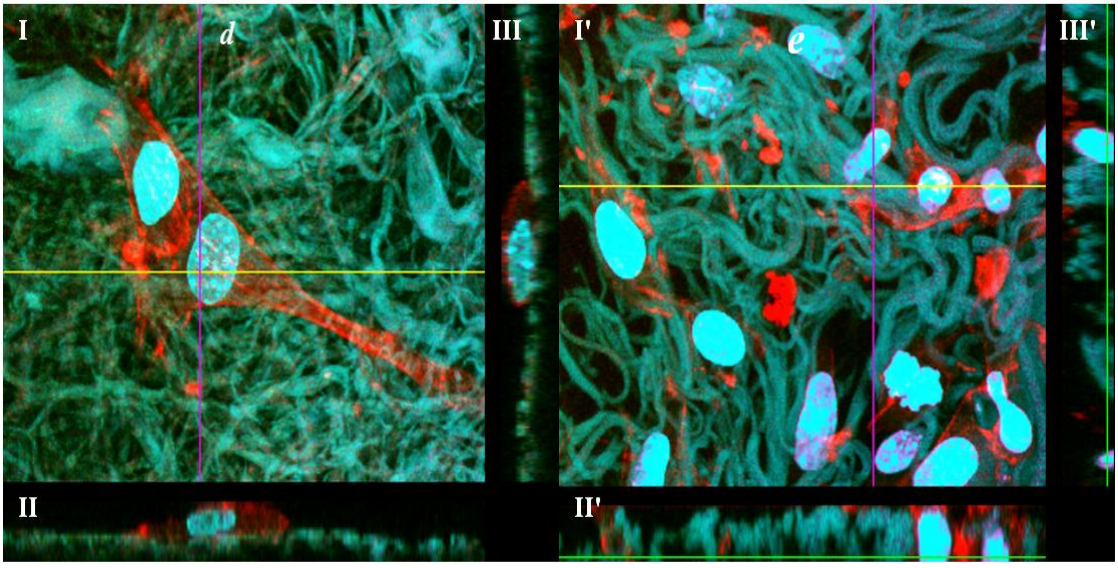
I
d
III
II
I'
e
III'
II'

Figure 15 a) MTS assay results of attachment (4 h) and proliferation (24 h, 72 h, 120 h and 168 h) of NIH 3T3 fibroblast cells on 2D and 3D zein electrospun scaffolds; b) 2D and c) 3D zein electrospun scaffolds of CLSM montage images in sequential sections at 10 μm intervals under magnification of 60x. The red network illustrated F-actin in NIH 3T3 cells stained with Phalloidin 633 at different depths from the surface after culture for 72 h; d) and e) CLSM images showing spreading of Phalloidin 633 and Hoechst 33342 stained NIH 3T3 cell on 2D and 3D zein electrospun scaffolds 48 h after seeding. Three dimensional reconstructions: xy projections (I and I'); xz projections (II and II'); and yz projections (III and III'). In all the figures, data labeled with the **same symbols** were **NOT** significantly different from each other.

What is more important, the spheroid-shaped three-dimensional cells on 3D scaffolds and flattened morphologies of cells on 2D scaffolds were shown in **Figure 15 d** and **e**. In **Figure 15 d.I**, the developed cytoskeletons of cells, which were indicated by the actin filaments stained in red, spread over the surface of 2D scaffold. As illustrated in xz projection in **Figure 15 d.II** and yz projection in **Figure 15 d.III**, thickness of the individual cell was much smaller than their planar sizes as shown in the xy projection. Cells seeded in the 2D scaffolds tended to grow into planar morphologies, which differed from that of cells *in vivo*. However, the side views of 3D scaffolds in **Figure 15 e.II'** and **III'** revealed that the same cells oriented in z direction rather than in x and y directions, since the lengths of cell nuclei in z direction were longer than the diameters of them in the xy projection. This result suggested that 3D scaffolds facilitated cells to develop into stereoscopic topographies that more closely mimic the cells in many native ECMs. It is of great potential that 3D regenerated tissues with satisfactory physiological morphologies and functions could be fabricated by integration of proper cells into the 3D electrospun scaffolds.

In Vitro Stem Cell Adipogenic Differentiation Study of Soyprotein Scaffold

5.8. *In Vitro* Stem Cell Adipogenic Differentiation Study of Soyprotein Scaffold

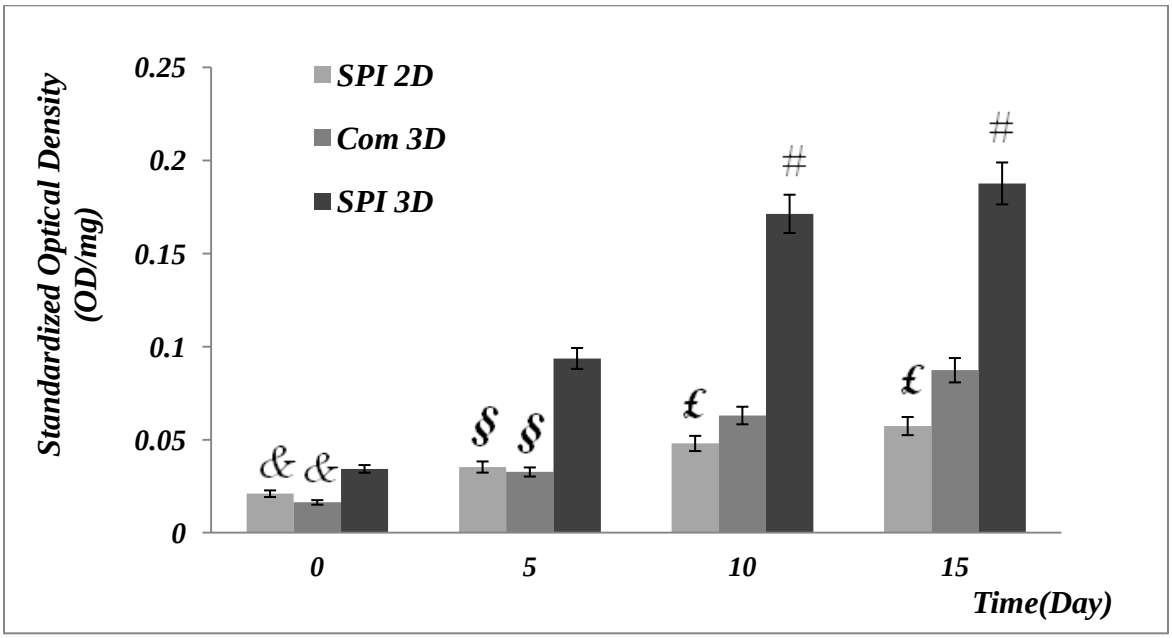

Figure 16 MTS assay results of attachment (0 day) and proliferation (5 days, 10 days, 15 days) of adipose-derived mesenchymal cells on 2D, 3D soyprotein electrospun scaffolds and on commercial **PCPU** (polycarbonate polyurethane-urea) 3D porous scaffold. In all the figures, data labeled with the **same symbols** were **NOT** significantly different from each other.

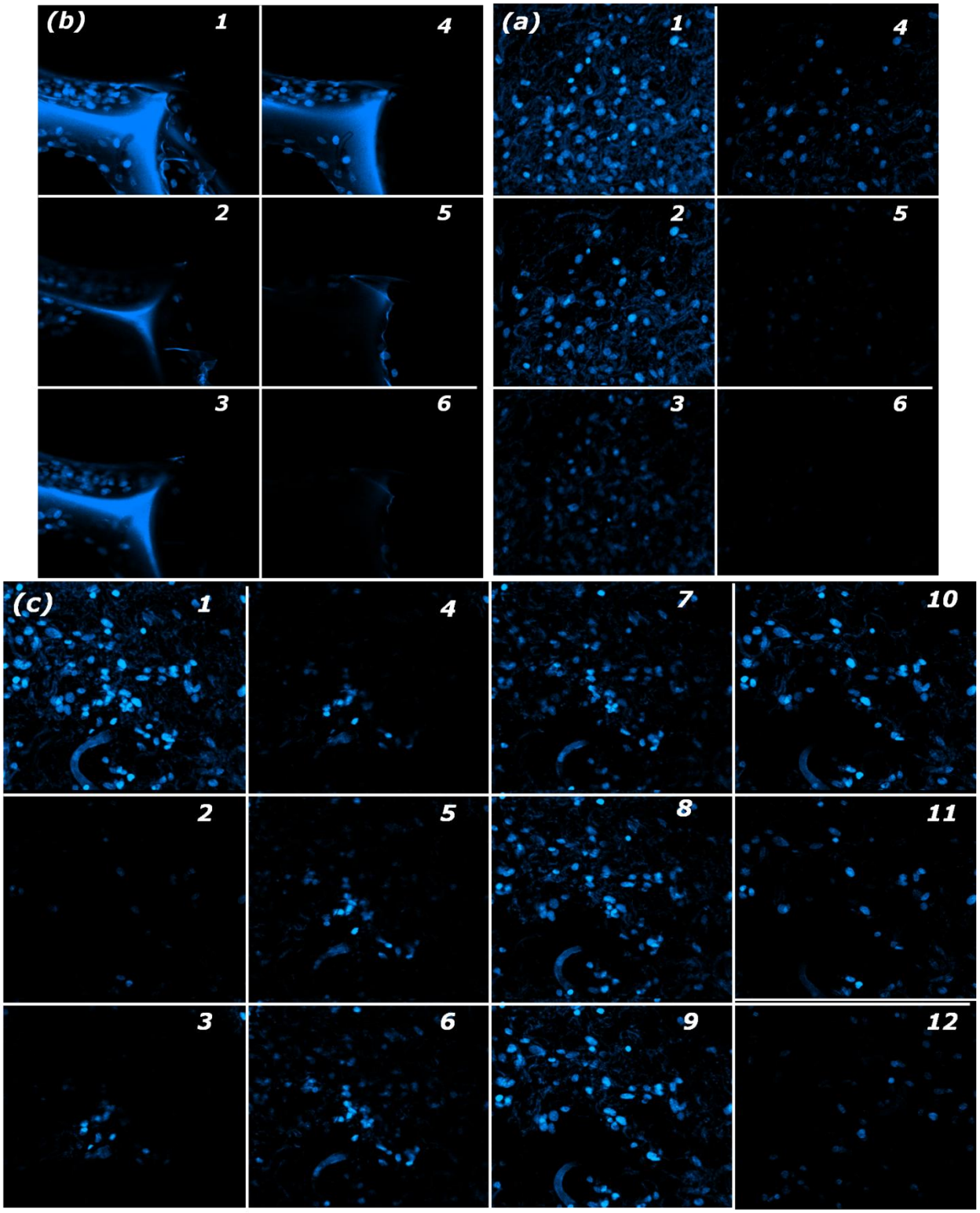

Figure 17 a) 2D and c) 3D soyprotein electrospun scaffolds, and b) commercial 3D porous scaffold of CLSM montage images in sequential sections at 15 μm intervals under magnification

of 60x. The light blue dots in the figure represent the cell nucleus stained with Hoechst 33342 dyes. The first pictures that labels with "1" in each figure are the combination of all the other pictures in the figure.

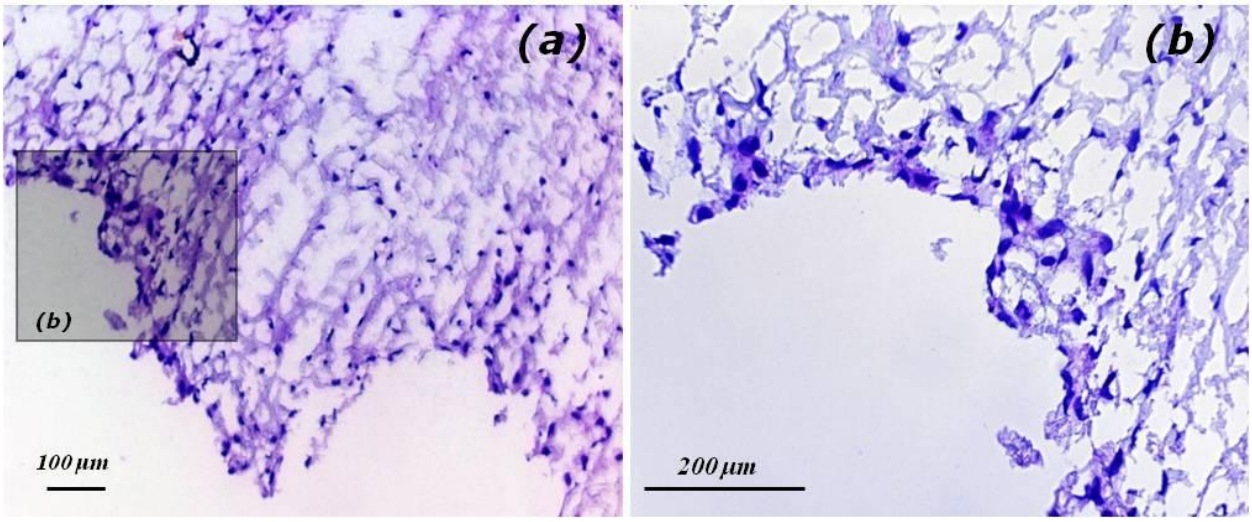

Figure 18 3D soyprotein scaffolds were collected at 15 days of culture, fixed in 4% phosphate-buffered formalin, embedded in paraffin, and cut into 0.5 mm sections and then were stained with H&E (Merck) to reveal the histological structure.

It can be found that, 3D soyprotein scaffolds were remarkably better than 2D soyprotein scaffolds and commercial 3D porous scaffold to support cell growth. As shown in **Figure 16.** More attachment and higher proliferation rates of ADMSC were found for 3D soyprotein fibrous scaffolds. The amount of cells attached on 3D scaffolds was 163% and 210% times of that on 2D scaffolds and commercial 3D scaffold. After cultured up for 2 weeks, the proliferation of cells on soyprotein 3D fibrous scaffolds was 227% and 114% higher than that on 2D scaffolds and commercial 3D scaffold at the same time point, respectively. The different cell culture results should be attributed to the differences of scaffold materials and to the cell accessibility induced by the differences in scaffold structure. The results were consistent with the observation in the

CLSM montage images in **Figure 17** and H&E staining images in **Figure 18**. After 1week of cell culture, cells were found at least 165 μm beneath the surface of 3D scaffold, while cells could not be found 45 μm under the surface of 2D scaffold. The tight packing of fibers in the 2D scaffolds restricted penetration of cells vertically, while the multiple pores with much larger size and significantly higher porosity of 3D scaffolds facilitated migration and penetration of cells into the interior of the structures.

For the commercial 3D porous scaffold, thought cell can still be observed below 75 μm under the surface of the scaffold, it should be noticed that the distribution of cells is highly uneven, and cells can only be found on the wall structure of the scaffold. The unevenly distribution of cells in commercial 3D porous scaffold may cause the formation of uneven soft tissue in long term *in vivo* soft tissue repairing process.

As a contrast, soyprotein 3D scaffolds facilitated migration and penetration of cells into the interior of the structures evenly, and shown the ability of soyprotein 3D scaffolds to support the formation of soft tissue in long term *in vivo* soft repairing process.

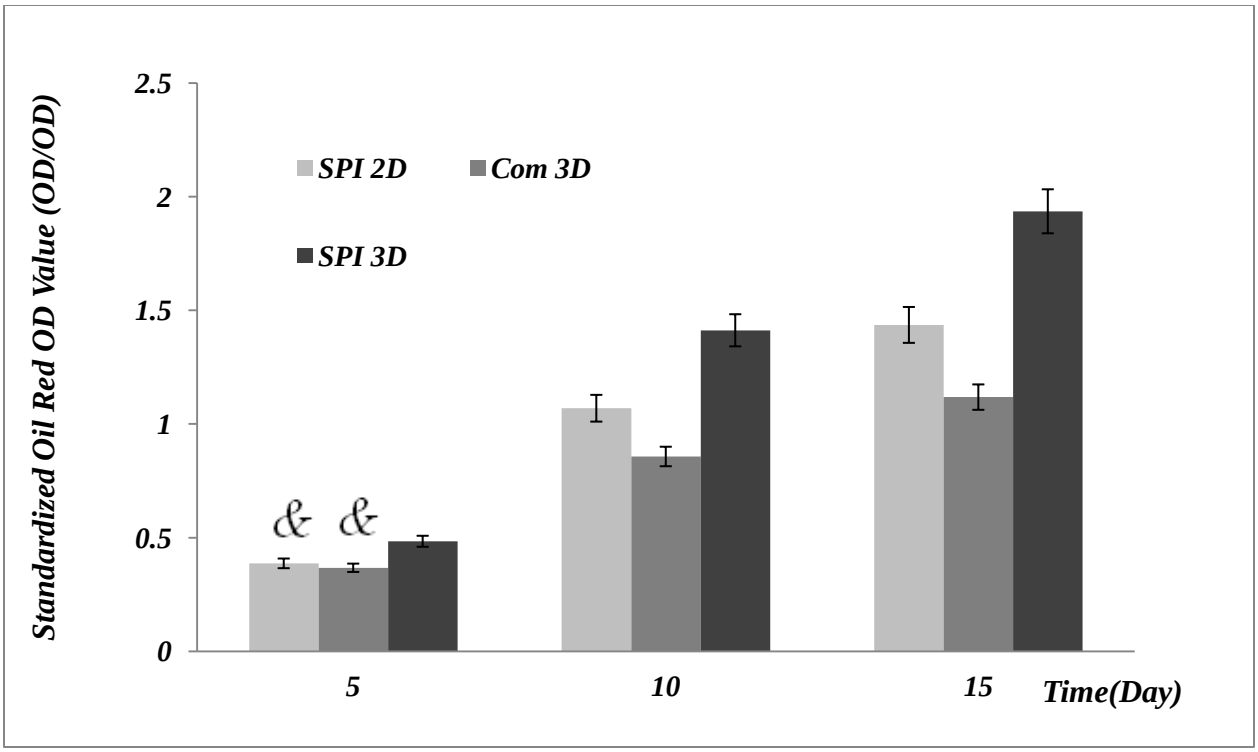

Figure 19 Adipogenic differentiation with different time intervals (5 days, 10 days and15 days) of ADSCs was analyzed by Oil red O staining. Cells were stained with Oil red O, destained with isopropanol, and the OD at 500 nm was determined. In all the figures, data labeled with the **same symbols** were **NOT** significantly different from each other.

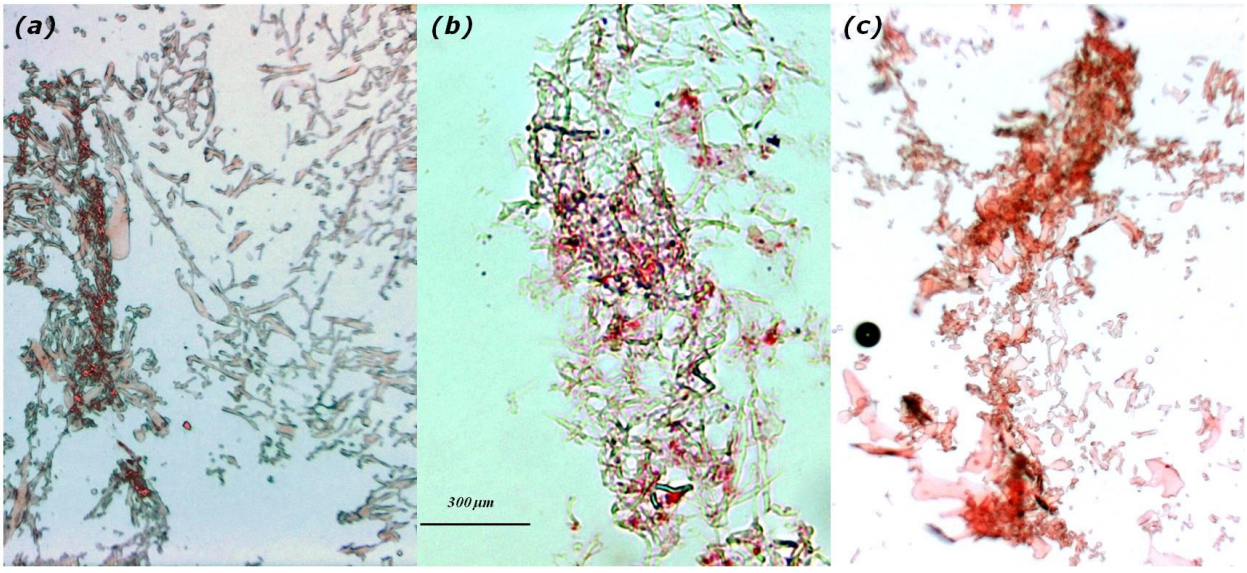

Figure 20 Oil red O staining of newly formed adipose tissue on a) 2D and c) 3D soyprotein electrospun scaffolds, and b) commercial 3D porous scaffold. Tissues retrieved from 3D soyprotein electrospun scaffolds showed substantially more tissue regeneration and adipogenic differentiation than tissues retrieved 2D soyprotein electrospun scaffolds and from commercial 3D porous scaffold.

Adipogenic differentiation was employed to test the ability to the three scaffolds for supporting soft tissue repairing. ADMSCS adipogenic differentiation was evaluated by staining with Oil red O. Oil red O is a lysochrome (fat-soluble dye) diazo dye used for staining of fat on paraffin sections. It has the appearance of a red powder with maximum absorption at around 500 nm. ADSCs was cultured in adipogenic medium for different time interval (5 days, 10 days and 15 days), and then stained with Oil red O solution, and finally destained in 100% isopropanol. The optical density (OD) of the solution was measured at 500nm using a UV/Vis multiplate spectrophotometer.

It can be found that, after cultured in differentiation medium for 15 days, the content of newly secreted fat by each ADMSC on soyprotein 2D fibrous scaffold was 28% higher than that on commercial 3D porous scaffold. This result showed that although more cells could be proliferated on commercial 3D porous scaffold, the differentiation degree of each ADMSC on soyprotein 2D fibrous scaffold was still higher than that commercial 3D porous scaffold. It proofed that soyprotein based scaffold could better support the adipogenic differentiation of ADMSCs, and consistent with the report that basal cell culture medium added soy peptides could significantly increase the proliferation of human adipose tissue-derived mesenchymal stem cells (ADSCs).

What's more, the content of newly secreted fat by each ADMSC on soyprotein 3D fibrous scaffold was 34% and 73% higher than that at on soyprotein 2D scaffolds and commercial 3D porous scaffold, respectively. For 2D and 3D soyprotein scaffolds were fabricated by the same raw materials, the difference of the oil red o OD value should be attributed to the difference of scaffold structure and fiber orientations. It is believed that a 3D randomly oriented fibrous environment is needed to guide cells to grow and differentiate into stereoscopic topographies, and cells cultured on flat 2D substrates may differ considerably in morphology and differentiation pattern from those cultured in more physiological 3D environments. Therefore, it could be concluded that the soyprotein 3D fibrous scaffold could better support ADMSC for adipogenic differentiation.

The results were also consistent with the observation in the Oil red O staining images in **Figure 20**. After 15 days of differentiation, a lot of fat tissues were found around 300 μm beneath the surface of 3D scaffold, while only a few fat tissues could be found 50 μm under the surface of 2D scaffold. For the commercial 3D porous scaffold, thought fat tissues can still be observed below 300 μm under the surface of the scaffold, it should be noticed that the darkness of the red color was much lighter than that on both 2D and 3D soyprotein scaffolds, which indicated that the stem cells on commercial 3D porous scaffold were not well differentiated, if compare to that on 2D and 3D soyprotein scaffolds. These result indicated that the soyprotein 3D fibrous scaffold could better support ADMSC for soft tissue repairing.

CHAPTER 6: CONCLUSIONS

In summary, a dissolution method was developed to extract soluble and spinnable soyprotein, and novel 3D zein and soyprotein electrospun scaffolds with three-dimensionally and randomly oriented fibers and large interconnected pores were successfully fabricated by reducing surface resistivity of materials.

The 3D scaffolds could better mimic naturally occurring 3D ECMs with spatially arranged and randomly oriented protein fibers. The morphologies of cells cultured in the 3D scaffolds could grow into stereoscopic morphologies that were more close to cells in the native ECMs. A mechanism, that increase in surface conductivity of material during electrospinning could induce formation of 3D electrospun structures, was proposed and validated.

The novel dissolution method could be applied to a number of water insoluble proteins which contains intermolecular and intramolecular disulfide bond crosslinkages, and 3D electrospinning method could be applied to a number of water insoluble proteins and many other water soluble materials.

In vitro cell attachment, proliferation and differentiation study indicated that the 3D fibrous scaffold could better support the attachment and proliferation of NIH 3T3 mouse fibroblast cells and adipose-derived mesenchymal cells, and could better support ADMSC for adipogenic differentiation.

CHAPTER 7: LITERATURE CITED

1. Shastri, V. P. Adv. Mater. **2009,** *21,* 3246–3254.
2. Bhattarai, N.; Li, Z. S.; Edmondson, D.; Zhang, M. Q. *Adv. Mater.* **2006,** *18*, 1463-1467.
3. Dvir, T.; Timko, B. P.; Kohane, D. S.; Langer, R. *Nat. Nanotechnol.* **2011,** *6*, 13-22.
4. Roskelley, C. D.; Desprez, P. Y.; Bissell, M. J. *P. Natl. Acad. Sci. USA.* **1994,** *91*, 12378-12382.
5. Yamada, K. M.; Cukierman, E. *Cell* **2007,** *130*, 601-610.
6. Smalley, K. S. M.; Lioni, M.; Herlyn, M. *In. Vitro. Cell. Dev-An.* **2006,** *42*, 242-247.
7. Bosman, F. T.; Stamenkovic, I. *J. Pathol.* **2003,** *200*, 423-428.
8. Bissell, M. J.; Rizki, A.; Mian, I. S. *Curr. Opin. Cell. Biol.* **2003,** *15*, 753-762.
9. Uygun, B. E.; Soto-Gutierrez, A.; Yagi, H.; Izamis, M. L.; Guzzardi, M. A.; Shulman, C.; Milwid, J.; Kobayashi, N.; Tilles, A.; Berthiaume, F.; Hertl, M.; Nahmias, Y.; Yarmush, M. L.; Uygun, K. *Nat. Med.* **2010,** *16*, 814-820.
10. Zegers, M. M. P.; O'Brien, L. E.; Yu, W.; Datta, A.; Mostov, K. E. *Trends Cell Biol.* **2003,** *13*, 169-176.
11. Petersen, T. H.; Calle, E. A.; Zhao, L. P.; Lee, E. J.; Gui, L. Q.; Raredon, M. B.; Gavrilov, K.; Yi, T.; Zhuang, Z. W.; Breuer, C.; Herzog, E.; Niklason, L. E. *Science* **2010,** *329*, 538-541.

12. Zhu, J.; Li, J.; Wang, B.; Zhang, W. J.; Zhou, G. D.; Cao, Y. L.; Liu, W. *Biomaterials* **2010,** *31*, 6952-6958.

13. Cukierman, E.; Pankov, R.; Yamada, K. M. *Curr. Opin. Cell. Biol.* **2002,** *14*, 633-639.

14. Griffith, L. G.; Swartz, M. A. *Nat. Rev. Mol. Cell. Bio.* **2006,** *7*, 211-224.

15. Lu, H. H.; Subramony, S. D.; Boushell, M. K.; Zhang, X. Z. *Ann. Biomed. Eng.* **2010,** *38*, 2142-2154.

16. Mikos, A. G.; Herring, S. W.; Ochareon, P.; Elisseeff, J.; Lu, H. H.; Kandel, R.; Schoen, F. J.; Toner, M.; Mooney, D.; Atala, A.; Van Dyke, M. E.; Kaplan, D.; Vunjak-Novakovic, G. *Tissue Eng.* **2006,** *12*, 3307-3339.

17. Saha, S.; Duan, X.; Wu, L.; Lo, P. K.; Chen, H.; Wang, Q. *Langmuir* **2012,** 28, 2028-34.

18. Haycock, J. W., 3D Cell Culture. **2011,** *695*, 1-15.

19. Huang, Z. M.; Zhang, Y. Z.; Kotaki, M.; Ramakrishna, S. *Compos. Sci. Technol.* **2003,** *63*, 2223-2253.

20. Li, D.; Xia, Y. N. *Adv. Mater.* **2004,** *16*, 1151-1170.

21. Hohman, M. M.; Shin, M.; Rutledge, G.; Brenner, M. P. *Phys. Fluids.* **2001,** *13*, 2221-2236.

22. Burger, C.; Hsiao, B. S.; Chu, B. *Annu. Rev. Mater. Res***. 2006,** *36*, 333-368.

23. Pham, Q. P.; Sharma, U.; Mikos, A. G. *Tissue. Eng.* **2006,** *12*, 1197-1211.

24. Nandakumar, A.; Yang, L.; Habibovic, P.; van Blitterswijk, C. *Langmuir* **2010,** *26*, 7380-7.

25. Debnath, J.; Brugge, J. S. *Nat. Rev. Cancer* **2005,** *5*, 675-688.

26. Hu, J.; Liu, X. H.; Ma, P. X. *Biomaterials* **2008,** *29*, 3815-3821.

27. Moroni, L.; Schotel, R.; Hamann, D.; de Wijn, J. R.; van Blitterswijk, C. A. *Adv. Funct. Mater.* **2008,** *18*, 53-60.

28. Yokoyama, Y.; Hattori, S.; Yoshikawa, C.; Yasuda, Y.; Koyama, H.; Takato, T.; Kobayashi, H. *Mater. Lett.* **2009,** *63*, 754-756.

29. Simonet, M.; Schneider, O. D.; Neuenschwander, P.; Stark, W. J. *Polym. Eng. Sci.* **2007,** *47*, 2020-2026.

30. Bonino, C. A.; Efimenko, K.; Jeong, S. I.; Krebs, M. D.; Alsberg, E.; Khan, S. A. *Small* **2012**, *8*, 1928-1936.

31. Jiang, Q. R.; Reddy, N.; Yang, Y. Q. *Acta Biomater.* **2010,** *6*, 4042-4051.

32. Ma, P. X. *Adv. Drug Delivery Reviews* **2008,** *60*, 184-198.

33. Birgersdotter, A.; Sandberg, R.; Ernberg, I. *Semin. Cancer Biol.* **2005,** *15*, 405-412.

34. Drury, J. L.; Mooney, D. J. *Biomaterials* **2003,** *24*, 4337-4351.

35. Ranney, M. W. *Antistatic agents: technology and applications, 1972*. Noyes Data Corp.: Park Ridge, N. J., **1972**; pp 113-162.

36. Cai, Y. Z.; Zhang, G. R.; Wang, L. L.; Jiang, Y. Z.; Ouyang, H. W.; Zou, X. H. *Journal of Biomedical Materials Research Part A* **2012,** *100A*, 1187-1194.

37. Hosseinkhani, H.; Hosseinkhani, M.; Hattori, S.; Matsuoka, R.; Kawaguchi, N. *Journal of Biomedical Materials Research Part A* **2010**, *94A*, 1-8.

38. Zhu, X. L.; Cui, W. G.; Li, X. H.; Jin, Y. *Biomacromolecules* **2008**, *9*, 1795-1801.

39. Beris, A.E., et al., *Injury*, **2005**. 36(4): p. S14-S23.

40. Huang, A.H., M.J. Farrell, and R.L. Mauck. *Journal of Biomechanics*, **2010**, 43, 128-136.

41. Li, W.J., et al. *Journal of Biomedical Materials Research Part A*, **2003**, 67A, 1105-1114.

42. Aung, T., et al. *Journal of Biomedical Materials Research*, **2002**, 61, 75-82.

43. Park, H., et al. *Biomaterials*, **2007**, 28, 3217-3227.

44. Sharma, B., et al. *Plastic & Reconstructive Surgery*, **2007**, 119, 112-120

45. Athanasiou, K.A., G.G. Niederauer, and C.M. Agrawal. *Biomaterials*, **1996**, 17, 93-102.

46. Cancedda, R., et al. *Matrix Biology*, **2003**, 22, 81-91.

47. Wang, Y., et al. *Biomaterials*, **2006**, 27, 6064-6082.

48. 11. Sando, L., et al. *Journal of Biomedical Materials Research Part A*, **2010**, 95A, 901-911.

49. Zoccola, M., et al. *Biomacromolecules*, **2008**, 9, 2819-2825.

50. Tachibana, A., et al. *Biomaterials*, **2005**, 26, 297-302.

51. Tachibana, A., et al. *Journal of Biotechnology*, **2002**, 93, 165-170.

52. Li, J., et al. *Journal of Biomedical Materials Research Part B*, **2012**, 100B, 896-902.

53. Sierpinski, P., et al. *Biomaterials*, **2008**, 29, 118-128.

54. Apel, P.J., et al. *The Journal of Hand Surgery*, **2008**, 33, 1541-1547.

55. Katoh, K., T. Tanabe, and K. Yamauchi. *Biomaterials*, **2004**, 25, 4255-4262.

56. Yamauchi, K., et al. *Journal of Biomedical Materials Research*, **1996**, 31, 439-444.

57. Tanabe, T., et al. *Biomaterials*, **2002**, 23, 817-825.

58. Tanabe, T., and K. Yamauchi. *Materials Science and Engineering: C*, **2004**, 24, 441-446.

59. Aluigi, A., et al. *European Polymer Journal*, **2011**, 47, 1756-1764.

60. Aluigi, A., et al. *Journal of Applied Polymer Science*, **2007**, 104, 863-870.

61. Aluigi, A., et al. *Journal of Biobased Materials and Bioenergy*, **2009**, 3, 311-319.

62. Aluigi, A., et al. *European Polymer Journal*, **2008**, 44, 2465-2475.

63. Li, J., et al. *Polymer Degradation and Stability*, **2009**, 94, 1800-1807.

64. Yuan, J., et al. *Macromolecular Research*, **2009**, 17, 850-855.

65. Erickson, G.R. *Biochemical and Biophysical Research Communications*, **2002**, 290, 763-769.

66. Zuk, P.A., et al. *Molecular Biology of the Cell*, **2002**, 13, 4279-4295.

67. Fainerman, V. B.; Möbius, D.; Miller, R. *Surfactants: chemistry, interfacial properties, applications*. 1st ed.; Elsevier Science, Ltd.: Amsterdam; New York, **2001**; pp 20-43